Asynchronous Inhibition in Neocortical Microcircuits

Tanya Sippy

Submitted in partial fulfillment of the
requirements for the degree
of Doctor of Philosophy
in the Graduate School of Arts and Sciences

COLUMBIA UNIVERSITY

2011

Abstract

Asynchronous Inhibition in Neocortical Microcircuits

Tanya Sippy

Neurons are constantly integrating information from external and internal sources, causing them to spike at particular times. The exact timing of spikes is determined by a neuron's intrinsic properties, as well as the interplay between local excitatory and inhibitory inputs. Although inhibitory interneurons have been extensively studied, their contribution to neuronal integration and spike timing remains poorly understood. To elucidate the functional role of GABAergic interneurons during cortical activity, we combined molecular identification of interneurons, two photon imaging and electrophysiological recordings in mouse thalamocortical slices. In this preparation, cortical UP states, a network state characterized by prolonged periods of depolarization and synchronized spiking, can be evoked by thalamic stimulation and can also occur spontaneously.

To assay the role of inhibition, we first characterized the firing properties of Parvalbumin (PV) and Somatostatin (SOM) interneurons during UP states activity, and found a higher probability and rate of spiking in these two subtypes compared to excitatory cells. These subtypes did not display differential timing of activation during the evoked response. Furthermore, calcium imaging showed low correlations among PV and SOM interneurons, indicating that neurons sharing these neurochemical markers do not coordinate their firing. Intracellular recordings confirmed that nearby interneurons, known to be electrically coupled, do not display more

synchronous spiking than excitatory cells, suggesting that this coupling may not function to synchronize the activity of interneurons on fast time scales. After characterizing inhibitory interneuron outputs, we next studied the timing and correlation of inhibitory *inputs*, which we isolated from excitatory inputs by voltage clamping at the reversal for excitation (0mV) or inhibition (-70mV). In both thalamically triggered and spontaneous activations, IPSCs between cell pairs were remarkably well correlated, with correlation coefficients reaching over .9 in some cases. This high degree of correlation has previously been assumed to be due to interneuron synchrony, but our population imaging and paired recordings did not support this view. In addition, we found that the connection rate between interneurons is very high (~80%), and quantal analysis revealed that each IPSC recorded in neighboring cells during an UP state could be due to a single presynaptic interneuron. Therefore, we explain the high IPSCs correlations in nearby pyramidal cells are emerging from the common input from individual interneurons, rather than from synchronization of interneuron activity across the population.

In a final set of experiments, we found that a partial pharmacological block of inhibitory signaling increased EPSC correlations. Our data support a model in which inhibitory neurons do not fire in a correlated fashion but have strong, dense connections to pyramidal neurons that serve to prevent local excitatory synchrony during UP states. This would mean that inhibition may not, as previously thought, serve to synchronize the firing of excitatory cells, but have precisely the opposite effect, decorrelating their activity by breaking down their coordinated firing. This is consistent with the hypothesis that pyramidal cells are carrying out an essentially integrative function in the circuit and that interneurons expand the temporal dynamic range of this integration.

Table of Contents

List of Figures

Acknowledgments

I wish to thank Rafael Yuste for guiding me through the world of imaging. I'd also like to thank him for giving me the opportunity to work in his lab, where I learned more than I thought possible during my PhD. Rafa, your advice that I should solve problems myself, keep the larger big picture in mind, and approach my thesis as a climb up a steep mountain made a lasting impact on me. I'll always be very proud to tell people I did my thesis work in your lab.

I'd also like to thank my committee chair, Larry Abbott, and the rest of the members, Bernardo Rudy, Steven Siegelbaum, and Charles Zuker. I am extremely lucky to have such a sharp, experienced group to provide me with feedback and encouragement.

Jason MacLean, who taught me the thalamocortical slice preparation, and also gave me exceptional feedback and guidance for years after he left the lab, even as an extremely busy starting professor.

Brendon Watson, whose well roundedness and ability to think about scientific problems from fine level detail all the way to the big picture was invaluable during my first few years of the lab. His exceptionally written thesis served as inspiration for my own.

Felix Schweizer, who was my mentor as an undergraduate, gave me my start in scientific research. I can only hope his passion, enthusiasm, and critical thinking skills will continue to influence me throughout my career.

All the members of the Yuste lab have been wonderful to work with. I'd especially like to thank those who worked on interneurons, Elodie Fino, Alan Woodruff and Adam Packer for stimulating discussions and productive collaborations. I'd also like to thank "little Laura", for her help and advice on various things, and sharing a lot of late nights and weekends with me in the lab. Ann Kennedy, a former rotation student in the lab has helped me a lot with understanding some theoretical work pertinent to my dissertation. Finally, a special thanks to Darcy Peterka, our resident expert on just about everything, for technical support with two photon imaging. I'm not sure there is anything Darcy *can't* do.

I've been fortunate to work with some highly talented collaborators, Joshua Vogelstein - who wrote the spike inference algorithm I used for my imaging analysis, Tim Machado- a MATLAB expert who gave me excellent pointers when writing code, and Rohit Prakash- whose energy and expertise in the world of optogenetics has been invaluable to me in the last few months of my dissertation.

I'm surrounded by highly talented, successful friends who add fun to my life, and are always there for me. Jessica, thanks for your generosity, and hospitality and also for editing this manuscript.

Beep, your support the past year really helped get me through; thanks for never doubting me. Dieter, you're awesome.

I cannot thank my parents enough for all they have done for me. Their selflessness and determination to do whatever they could so I could focus completely on my course of study is the primary reason I've been able accomplish anything during my academic career.

And finally, I want to thank my sister, who has been with me every step of the way throughout this MD/PhD journey here in New York, and whose support and tolerance is never ending.

Dedication

To my two great parents, and sister, Sujeeta.

Preface

When I was younger (and admittedly a little bit to this day), I didn't understand how people could want to be anything but scientists. Science is the study of the world around us, and who wouldn't want to spend their lives understanding how the world works?

The overall goal of science, to explain the origin of the universe and the rules that govern it, represents the most challenging and complex task of human intellectual pursuit. One could argue that in order to approach this undertaking, it makes sense to proceed chronologically in the order in which life itself was established, beginning with properties of our solar system, and ending with our biology. But how we perceive our world depends on the very tool we use to decipher it, our brains. For me, at the heart of all scientific knowledge is the question of how our brains reconstruct reality, and this is why I chose to focus on the field of neuroscience.

The brain is composed of millions of individual cells, or neurons. These cells contain the same genetic makeup as the cells in the rest of our body, yet individually and in combination they possess the extraordinary properties that allow us to think and feel. Therefore, the hope and the challenge before us is to gain some fundamental insight into how neural cells perform these remarkable feats of function. How do neurons, biological structures made of organic and inorganic molecules and proteins, give rise to thoughts, sensations, feelings and actions?

While there exists a number of ways to approach these questions, for the past five years I have chosen to study the cortical microcircuit. The cortex is the outermost part of the brain, composed of neuronal cell bodies, which play a key role in memory, attention, perception,

thought, language, and consciousness. A microcircuit is a collection of neurons within the cortex that together carry out a particular function. By concentrating on just a few hundred cells at a time in a local region, we are using a reductionist approach to determine a fundamental feature of brain function- processing of information. What can the activity of neurons tell us about how they encode information? What is the function of particular neurons within the cortical microcircuit? These two questions form the basis of my dissertation. I describe my work with caution and humility, based on my appreciation of the complexity of the brain and my recognition of the limits of our understanding of neural function, especially in neocortex.

Chapter 1- Introduction

Studying the brain at the circuit level

In attempting to bridge the gap between individual neurons and whole brain function, it is useful to consider the various levels of complexity that build on each other in the brain. The state of neuroscience, viewed at a macro-level, shows a hierarchy of complexity from the molecular functions within synaptic junctions (and associated glial cells) through the workings of whole neurons, through circuits of neuronal assemblies, all the way up to the functioning of whole brains comprised of intercommunicating modular regions. One could make the argument that in order to fully understand information processing at any one of these levels, you must first understand completely each preceding level of organization. However, it has been demonstrated in many examples of human study that an understanding of the details at the lower levels is not necessary to describe higher levels; humanity was able to learn about chemistry even while treating it as a separate field from physics, in spite of the fact that physics underlies all chemical phenomena. Similarly, biology may be studied without understanding all of its chemical underpinnings. Therefore, a given phenomenon can be considered to be an emergent property of its underlying processes, and understanding the details of these processes may not be necessary for studying the phenomenon itself.

Due to many layers of complexity in the brain, it is a daunting task for a neuroscientist to decide where to focus his/her efforts. While some of us focus on work at the level of just one or a few neurons, others work on interpreting signals from entire brain areas, while still others work primarily on behavior. Although each of these areas is fundamentally important to understanding

how the brain functions, the body of work described in this doctoral thesis is aimed at the intermediate level between the single neuron and the behaving organism—the neural circuit.

Neurons receive input from other neurons and integrate these inputs depending on a variety of membrane and channel based properties (Lorente de No and Condouris, 1959; Rall, 1959; Yuste and Tank, 1996) which can vary greatly depending on the neuron type (see section on neuronal subtypes below). If the sum of these inputs is large enough, the neuron will reach threshold and fire an action potential, which will result in an input in the next downstream set of "postsynaptic" neurons (Adrian, 1914; Brock et al., 1952; Coombs et al., 1955; Diamon and Yasargil, 1969). This recursive process forms the basis of mental functions such as thought, perception and consciousness, and represents the biological underpinning of the mind (Kandel, 2006). Although we now understand this basic method of communication between cells, we still do not know how groups of neurons work together to accomplish relatively simple tasks, such as grasping for a cup, let alone complex abstract thoughts. Such tasks are unlikely to be the sum of individual neurons, but rather a collective, or emergent property of neuronal and synaptic integration.

Surprisingly, our knowledge of the brain at the circuit level is quite scant. We have a good underpinning of its neuroanatomy of the brain at both the macro and micro levels. Thanks to the field of neuropsychology, which attempts to identify the area of the brain important for particular cognitive tasks, we have made some macroanatomical correlates of brain function (Adrian, 1941; Brodmann, 1999; Felleman and Van Essen, 1991; Kwong et al., 1992; Marshall et al., 1937; Penfield and Rasmussen, 1950). In addition we have some comprehension of the critical mechanisms of synaptic communication (Del Castillo and Katz, 1954, 1955; Fatt and Katz, 1952),

and integration (Brock et al., 1952; Coombs et al., 1955; Diamon and Yasargil, 1969), albeit with many holes. However, we have remarkably little knowledge regarding how the coordinated activity of many neurons leads to macro level brain function. Arguably, we know more about higher order phenomena such as psychology and behavior than we know about the integrated properties of neuronal ensembles that underlie these functions.

For all the reasons outlined above, it is crucial that we use the tools made available recently, many of which have been fully or partially developed in the Yuste lab, where I have done my research for this thesis, to study the properties of neuronal circuits. This dissertation focuses on understanding properties of neurons when they are activated (fire action potentials) in a coordinated manner.

The cortex: from structure to function

The neocortex, or more simply "cortex" is the outermost wrapping of the brain. It is composed of billions of neurons, which make trillions of connections like a complex web. This area of the brain is important for most complex tasks and thoughts (Damasio, 1994; Weinberger et al., 1986) which is why it is an intriguing, albeit sometimes frustrating, structure to study. One clear organizing principle that emerged in the 19th century is that different areas of the brain are dedicated to processing diverse streams of information (Broca, 1861). Within these areas, the picture can be more refined. In somatosensory cortex, for example, the location of cells corresponds to the part of the body from which they receive sensory inputs (Adrian, 1941); adjacent parts of the body are represented by nearby cells, creating a full map of the body on the surface of the cortex.

Large progress was made in understanding the finer structure of the cortex in the 1950s and 1960s by David Hubel and Torsten Wiesel. Their studies in cat visual cortex with single unit recordings revealed that neurons respond to specific visual cues, in particular the location and orientation of lines in specific portions of the visual field (Hubel and Wiesel, 1959). Perhaps the most significant part of their contribution was that neurons within a particular "column" of cortex (defined as a cylindrical group of cells extending through all the 6 layers or cortex) responded to similar stimuli. Their work, together with Mountcastle and Lorente's previous studies, therefore proposed the cortical column as a structural and computational unit of the brain, an idea that continues to be highly influential among neuroscientists studying structure/function relationships in cortex. [1]

In the 1980s Gilbert and Wiesel were able to lay out a scheme for the general flow of information through a cortical column (Gilbert and Wiesel, 1983): input to the cortex from thalamus enters layer IV (Gilbert and Wiesel, 1983), flows to layers II and III (Beierlein et al., 2003; Petersen et al., 2003a; Shepherd et al., 2003) and from there is sent to layer V (Staiger et al., 2000). In this model, layer connectivity occurs within a single cortical column, providing a three dimensional framework of layers and columns fundamental to cortical function. Each column essentially operates as an independent processing unit, performing computations on different aspects of incoming data (Mountcastle, 1978).

[1] Although this work has laid the foundation for many subsequent studies relating cortical structure to function, it is not clear how generally applicable the organization into columns is across cortical areas and species (Horton and Adams, 2005).

The general organizing principals established in the visual system have been shown to be true in another sensory cortical regions, the rodent whisker somatosensory cortex.

This area has been referred to as the “glomerular” (Lorente de No, 1922b) or "barrel cortex" (Woolsey and Van der Loos, 1970) because of its clear columnar organization in which each "barrel" (easily distinguished after cytochrome oxidase staining), receives and processes data primarily from one whisker (Welker, 1976). The fundamental map of cortical information flow laid out by Gilbert and Wiesel has held up in this system (Feldmeyer et al., 2002; Land et al., 1995; Lubke and Feldmeyer, 2007; Reyes and Sakmann, 1999). This system, which has proven very useful for cortical neuroscientists, was used to perform all the experiments described in this thesis.

Cell Types in Cortex: many structures without a function

Beyond the macro structure of the cortex, electrophysiological and morphological studies of individual cells have revealed another level of organization in the cortex: cellular classes (Gupta et al., 2000; Lorente de No, 1922b; McCormick et al., 1985; Ramón y Cajal et al., 1988). In all cortical areas in mammals, there exist two broad subclasses: 1) excitatory pyramidal, or principal cells and 2) a variety of inhibitory interneurons. (Gupta et al., 2000; Lorente de No, 1922b; McCormick et al., 1985; Ramón y Cajal et al., 1988). These cell types have been studied and classified based on their morphologies, cellular and molecular characteristics, and intrinsic membrane properties. More recently, much attention has been given to their relative abundance in cortical layers, and to establishing their specific connectivity schemes within and across layers (Fino and Yuste, 2011; Gupta et al., 2000; Kampa et al., 2006; Kätzel et al., 2010; Lorente de No,

1922b; McCormick et al., 1985; Ramón y Cajal et al., 1988; Yoshimura and Callaway, 2005; Yoshimura et al., 2005) .

What is missing, though, is how cell types contribute to the function within this microcircuitry. What we do know is that most principal neurons within the central nervous system are “excitatory”, that is they mainly use the neurotransmitter glutamate to make the propagation of signals more likely in their downstream targets. Inhibitory cells, on the other hand, use the neurotransmitter GABA to shunt excitatory inputs in their downstream cells, making signal propagation less likely. However, beyond the most rudimentary textbook description that excitatory neurons excite their downstream postsynaptic partners, while inhibitory cells do the opposite, we know surprisingly little about what role these cell types play in information processing. Inhibitory interneurons are especially daunting, since they are an extremely diverse group. The ability to probe the activity of these cell types within local circuits may be the best way to begin to untangle their function.

Inhibition in neocortex

Understanding the structure-function relationships of inhibitory interneurons and GABAergic circuits represents one of the major challenges in contemporary neuroscience. One reason for this is that, until recently, studies of interneurons have lagged behind those of excitatory principal neurons. This is due in part due to the fact that glutamatergic neurons far outnumber interneurons, making them easier targets for investigation. Due to new techniques designed which have increased the feasibility of identification and recording of interneurons in

vitro (Stuart et al., 1993) and in vivo (Monyer and Markram, 2004), an astonishing amount of variability within the interneuron population has been revealed.

Inhibitory interneurons, which comprise 10-20% of all cortical neurons, display enormous diversity in their anatomical, physiological, molecular, and synaptic properties (Freund and Buzsaki, 1996; Gupta et al., 2000; Kawaguchi et al., 1997; Lorente de No, 1922a). Although some attempts have been made, classification of interneurons based on these features continues to be a major issue in interneuron research (Ascoli et al., 2008; Markram et al., 2004). The functional implications of these classification schemes are even harder to elucidate, but one major classification rule has been observed thus far: interneurons that target different compartments of their postsynaptic targets have discrete effects on their downstream partners (Buhl et al., 1994; Miles et al., 1996; Somogyi et al., 1998). For example, interneurons targeting the perisomatic region are thought to control the output of downstream targets (Cobb et al., 1995; Freund and Katona, 2007). In sensory systems, it has been shown that fast spiking interneurons, which target peri-somatic regions, are instrumental for determining the spike timing of their excitatory targets. This 'feedforward inhibition' results from powerful and fast thalamic synapses onto GABAergic cells, and functions to narrow the amount of time over which downstream excitatory cells can produce action potentials (Mountcastle and Powell, 1959; Pouille and Scanziani, 2001). On the other hand, interneurons that innervate pyramidal cell dendrites are responsible for the control of the efficacy and plasticity of inputs from sources that terminate in the same dendritic domain (Buhl et al., 1994; Freund and Katona, 2007). Dendritic inhibition may also control the communication between dendrites and soma by shunting co-aligned excitatory inputs and modulating back-propagating action potentials (Mann and Paulsen, 2005). Finally, neurons

belonging to a subtype of dendritic targeting interneurons have been shown to be reliably recruited with activity of just one or a few upstream pyramidal cells in layers and are thought to be important for 'feedback inhibition' (Kapfer et al., 2007; Kozloski et al., 2001; Silberberg and Markram, 2007).

In spite of decades of investigations, it is still unknown exactly what inhibition does in the cortex, and it is unclear how the differential effect of interneuron subclasses on postsynaptic targets translates to their function within neural circuits. Traditionally, the function of GABAergic interneurons has been described as simply providing balance to excitation in order to prevent overactivity. While this is undoubtedly true, it is now apparent that the picture is much more complex. A flurry of recent work has provided evidence that inhibitory interneurons shape the activity of and control the precise timing of entire groups of principal cells (Cobb et al., 1995; Monyer and Markram, 2004). In cortex, network oscillations represent the collective activity of large neuronal populations, vary in frequency depending on the behavioural state of the animal, and are considered to be important for a variety of higher cognitive functions (Buzsaki and Draguhn, 2004; Duzel et al., 2010; Klausberger et al., 2003; Lisman and Buzsaki, 2008). An increasing body of work provides evidence in support a central role for interneurons in generating these phenomena (Blatow et al., 2003; Buzsaki and Draguhn, 2004; Cobb et al., 1995; Freund and Katona, 2007; Howard et al., 2005; Klausberger et al., 2003; Mann and Paulsen, 2005; Mann et al., 2005; Somogyi and Klausberger, 2005; Whittington and Traub, 2003). Recently, however, this view has been challenged by work demonstrating that interneurons that normally display correlated firing and synchronous

activity, can become rapidly and strong desynchronized in response to synaptic inputs, and impart this desynchronization onto the local network (Vervaeke et al., 2010).

While these studies are compelling and informative, they leave a large gap in our understanding of the function of interneurons. They have demonstrated the effect of interneurons at individual synapses, and at the other end of the spectrum, shown a role for them in oscillations of large ensembles. However, we still do not know what GABAergic interneurons do in *local* cortical circuits. We don't even know if interneurons belonging to a specific subclass have activity that is more similar to one another than to other cells. If they did, it would suggest they could have similar response properties to stimuli, and carry out their function in a coordinated manner. We also do not know what role interneurons have in sculpting the response of principal neurons during ongoing cortical activity. Finally, it is unclear whether different types of interneurons have differential roles in determining distinct dynamics of the circuit response. These are the fundamental questions forming the basis of and inspiration of my research.

Neurochemical markers of interneurons

Over the past 15 years, techniques to genetically label particular neuronal populations have facilitated the study of interneurons. Inhibitory interneurons release the neurotransmitter GABA, which is synthesized via a pathway involving the enzyme glutamic acid decarboxylase (GAD). This has been utilized in the creation of transgenic mouse lines in which expression of enhanced GFP (EGFP) is driven by either the GAD65 (Lopez-Bendito et al., 2004) or GAD67

promoter (Tamamaki et al., 2003), allowing fluorescence-aided identification of GABAergic interneurons.

Since interneurons are far from homogeneous in their function, GAD67 is not ideal for studying a particular class of interneurons. Fortunately, a number of neurochemical markers, including parvalbumin and somatostatin, are preferentially expressed in relatively discrete interneuron populations.

Interneurons that express parvalbumin (PV) have a predilection for synapsing on proximal portions of their target cell (Kosaka et al., 1987). These neurons can be further subdivided into those forming a basket-like plexus around the soma and proximal dendrites of principal neurons and those forming a row of boutons running alongside the axon initial segment of principal neurons (Freund and Buzsaki, 1996), These two cell types have been named 'basket' and 'chandelier or axo-axonic' cells, respectively, although some exceptions exist in cortex (Blatow et al., 2003). Neurons containing PV are by far the most numerous accounting for approximately 40% of all GABAergic interneurons in mouse neocortex (Xu et al., 2010).

Somatostatin (SOM), on the other hand, is a neuropeptide that is expressed in interneurons that show broader heterogeneity than parvalbumin positive cells. It is generally agreed that somatostain positive interneurons target the distal dendrites of their postsynaptic partners (Katona et al., 1999; Kawaguchi and Kondo, 2002), but in somatosensory cortices, these neurons can target peri-somatic regions as well (Markram et al., 2004). Recent work has identified three groups of SOM interneurons, based on their anatomy and physiology. The most abundant of these are the 'Martinotti cells,' in layers 2/3 through 5 of somatosensory cortex

which have ascending axons that branch in layer 1 (McGarry et al., 2010). About 30% of interneurons in the brain express SOM (Rudy et al., 2011).

Fortunately, due to the presence of these PV and SOM molecular markers, transgenic mouse lines in which PV or SOM interneurons are labelled with green fluorescent protein have been made (Chattopadhyaya, 2004; Oliva et al., 2000). These two mouse lines have aided the study of interneurons belonging to these subtypes, and enabled the work presented in this thesis.

Cortical UP states

In order to study the role of cortical interneurons, it is necessary to study them during an *active* circuit, that is one where neurons are either spontaneously firing action potentials or fire them in response to a stimulus. Cortical UP states are defined as the coordinated activation of large groups of cells lasting anywhere from a few hundred milliseconds to seconds, depending on the species and preparation in which they are observed. UP states were first described in 1981, when they were noted in intracellular recordings in the basal ganglia in vivo (Wilson and Groves, 1981), but had never been observed to occur coincidently with any sort of patterned multicellular activations. UP states are depolarized periods during which action potentials occur and in which *in vivo* systematically and semi-regularly alternate with "DOWN states" during which neurons are relatively hyperpolarized and do not generate action potentials. They are most frequently observed to occur in cortical neurons under anesthesia (Wilson and Kawaguchi, 1996) and during slow wave sleep (Steriade et al., 2001). Furthermore, it appears that UP states originate in the neocortex and drive either UP states or related activity in other parts of the forebrain including widely across the cortex (Arieli et al., 1996; Isomura et al., 2006), the basal ganglia (Mahon et al.,

2001) and hippocampus (Hahn et al., 2006, 2007; Isomura et al., 2006). It is conceivable that cortical UP states entrain all of the forebrain to the rhythm of the cortex itself during slow wave sleep. Indeed, recent work indicates that UP states can be coordinated across larger cortical territories (Hahn et al., 2007) and it has even been suggested that they represent the substrate for the “resting state” activity in fMRI (Fox et al., 2007).

During UP states, the spatial distributions and temporal activation patterns of the coactive neurons have some degree of repeatability from event to event, suggesting the potential importance of these activations (MacLean et al., 2005). When neurons are patch clamped for intracellular recording of their membrane potentials, plateau-like depolarizations are observed, lasting approximately 2 seconds, during which action potentials may be fired (Cossart et al., 2003; MacLean et al., 2005). Based on the fact that the multi-neuronal activations observed during UP states are synchronous and appear to occur among specific groups of neurons, they appear to be the sorts of coactive cortical neuronal ensembles that could be particularly informative of how inhibitory cells may function within cortical circuits. Thus, UP states are the substrate upon which the studies in this thesis are based upon. For the remainder of this dissertation cortical coactivations occurring during UP states will be referred to either simply as “activations” or "ensemble activations".

Chapter 2- Materials and Methods

Slice preparation

Thalamocortical slices, 400 μm thick, were prepared from postnatal day 13 (P13) to P18 from GIN (Oliva et al., 2000) or G42 (Chattopadhyaya, 2004) transgenic mice, as previously described (MacLean et al., 2005). Slices were cut with a vibratome (VT1200S; Leica, Nussloch, Germany or Microm 650V, ThermoFisher Scientific, Kalamazoo, Michigan) in ice-cold oxygenated modified ACSF that included 0.5 mM $CaCl_2$ and 3.5 mM $MgSO_4$, in which NaCl was replaced by an equimolar concentration of sucrose. Experiments were performed with ACSF containing (in mM) 123 NaCl, 3 KCl, 26 $NaHCO_3$, 1 NaH_2PO_4, 2 $CaCl_2$, 2 $MgSO_4$ and 10 dextrose, which was continuously aerated with 95% O_2, 5% CO_2. All experiments were performed in the absence of any ionic or pharmacological manipulations (with the exception of GABAzine in 100-200nm concentrations for one set of experiments shown in figure 14) but with high perfusion and oxygenation rates.

Electrophysiology

Thalamocortical projection neurons were activated using bipolar platinum-iridium electrodes (#CE2C55, Frederick Haer Co., Bowdoinham, ME) placed in the ventrobasal nucleus (VB) of the thalamus. Stimuli were 200 μs in duration, 20-100 μA in amplitude and were applied individually or as a train of 4 - 8 stimuli, each separated by 25 ms (40 Hz) using a Master 8 pulse

generator coupled to a Iso-flex stimulator (AMPI, Jerusalem, Israel). For each slice the minimal pulse amplitude necessary to evoke recurrent activity was used which allowed us to minimize potential activation of corticothalamic neurons (Agmon and Connors, 1991; Ferster and Lindstrom, 1985). Recordings were made at either 37º C or at room temperature and results were pooled since no differences were observed between data collected at these two temperatures. Calcium imaging of populations of neurons (Yuste and Katz, 1991) was used to identify online responding cells in layer 4 and these neurons were then targeted for whole-cell recording. Whole-cell current-clamp recordings Multiclamp 700B amplifiers (Axon Instruments, Foster City, CA) were made from neurons in layer 4 using 4-6 MΩ micropipettes, filled (in mM): 130 K-methylsulfate, 2 $MgCl_2$, 0.6 EGTA, 10 HEPES, 4 ATP-Mg, and 0.3 GTP-Tris, pH 7.2 (290-295 mOsm). To characterize neurons, 500-1000ms depolarizing DC current injections were given to each cell and resultant action potential firing patterns were analyzed, following the Petilla convention nomenclature (Ascoli et al., 2008).

Morphological processing

Neurons were filled with biocytin by diffusion from the intrapipette solution during recordings, with electrodes containing 0.4 g/100ml biocytin in addition to the solution described above. At the end of each recording, slices were fixed overnight in 4% paraformaldehyde. Thereafter, slices were rinsed several times in 0.12 M phosphate buffer saline (PB). Slices were then transferred to 30% sucrose in 15 mL of 0.12M PB for at least 2 hours and as long as one week. Slices were then frozen in an embedding medium. After freezing, slices were rinsed in 0.12M PB several times. Slices were then incubated in 1% H_2O_2 in 0.12M PB for 30 minutes under

agitation and rinsed in 0.12M PB once for 15 minutes. After two other washes in 0.02M KPBS, the slices were incubated overnight under agitation in 1% Avidin-Biotin Complex (ABC Kit Standard, Vector Laboratories) prepared in 0.3% Triton X-100. After three rinses in phosphate buffer, biocytin was revealed by diaminobenzidine. After two final rinses in phosphate buffer, slices were mounted onto slides. The neurons were reconstructed with Neurolucida (Micro Bright Field Inc., USA).

UP state detection

UP states were detected automatically (based on an algorithm written by BO Watson) from whole cell current clamp traces based on fulfillment of the following minimum criteria: at least 500 ms of depolarization of 3 mV or more and at least 3 action potentials during this depolarization. If the neuron did not fire action potentials, a continuous depolarization of 5 mV for a minimum of 500 ms was required. This allowed us to detect all UP states despite the variability of membrane behavior exhibited by different neurons. Simultaneous patch clamp recordings confirmed that these criteria allowed for the reliable detection of network UP state events which occurred simultaneously in simultaneously recorded cells. Further, after automatic detection, all events meeting these requirements were reviewed by the experimenter and could be rejected at that point. Durations and amplitudes for verified UP states were quantified based on automatically detected UP state start times and stop times. Action potentials were detected based on their amplitudes and durations and numbers within detected UP states were quantified.

Calcium indicator bulk loading and imaging

Slices were bulk loaded with Fura 2-AM for visualization of action potential-related activity in neuronal somata. Slices were placed onto the bottom of a small Petri dish (35 x 10 mm) filled with a vortexed mixture of 2 ml ACSF, an aliquot of 50 µg Fura 2-AM (Molecular Probes), 15 µl DMSO and 2 µl Pluronic F-127 (Molecular Probes). A cover was placed over the petri dish and it was incubated in the dark at 35–37 °C and oxygenated by puffed CO2/O2 gas for ~25 minutes. In order to locate regions in the cortex connected to the area of thalamus we stimulated, we first imaged at low (4X) magnification. Barrels were identified in bright field as repeating 'hollow rectangles', corresponding to regions of high cell density, occurring in layer 4, as confirmed with cytochrome oxidase staining (e.g (Feldmeyer et al., 1999). The region in the barrel fields which responded earliest to stimulation was then chosen for higher cell resolution imaging and patch clamping.

Changes in intracellular free Ca2+ were visualized with a 'fat' 20x (NA, 0.95) Olympus Plan FL objective with an upright fluorescence microscope (Olympus BX50WI; Olympus Optical, Tokyo, Japan) using a Ti:sapphire laser (Chameleon Ultra II, Coherent, >3 W, 140 fs pulses, 80 MHz repetition rate) tuned to either 790 (fura-1 AM imaging) or 900nm (GFP imaging). A Hamamatsu C9100-12 (Bridgewater, NJ) camera and Micro-Manager (Vale Lab, UCSF) and Image J software (a public domain, Java-based image processing program developed at the National Institutes of Health) were used for targeting neurons for imaging activity from populations of

neurons. Frames were acquired at 15-15.67ms/frame. Binning was performed such that images were 256x256 pixels. Files were saved as multipage tiffstacks.

First, a slow raster scan was performed at a low frame rate (1Hz) to identify cell bodies. In G42 and GIN transgenic knockin mice, the GABAergic GFP labeled interneurons were excited at 900nm. Subsequently, the same field was imaged at 790nm to visualize loaded cell bodies. After these imaged were acquired with the camera, neurons were targeted for imaging on their cell bodies, using a spatial light modulator (SLM). We use a model 1080P phase SLM from Holoeye (Berlin, Germany), which has a resolution of 1920 × 1080 pixels, and an 8-bit phase quantization, with a 60-Hz refresh rate. Patterns were generated with software from Holoeye. In our microscope, collimated light from our laser passes through an optional Pockels cell, which regulates total power, and after beam reshaping and resizing, hits the reflective SLM. A system of lenses relays the image of the SLM surface to the back aperture of the main microscope objective. Some small fraction (<25%) of the incoming light remains undiffracted – this is the "zero-order" beam. We used an "on-center" configuration wherein the non-diffracted beam is present in the FOV, and we employ a small beam-stop to remove it.

Image analysis

To detect calcium signals from imaged cells, loaded neurons were automatically identified using a custom written Image J plug-in (TA Machado) on the raw image of the slice, and then the fluorescence of these cells was measured as a function of time. All remaining image processing was carried out using custom written software in MATLAB (The MathWorks, Inc., Natick MA).

Fluorescence traces were then preprocessed. Because some slow drift was sometimes present in the traces, each trace was Fourier transformed, and all frequencies <0.5 Hz were set to zero (0.5 Hz was chosen by eye); the resulting fluorescence trace was then normalized to be between zero and one. Taking advantage of the high temporal resolution of our data, we employed a fast nonnegative deconvolution algorithm (Vogelstein et al., 2010) to infer the approximately most likely spike train underlying our fluorescence data. Briefly, the algorithm uses a model that assumes somatic fluorescence arising from the calcium indicator is the convolution of the neuron's spike train and an exponentially decaying kernel. Noise is assumed to be gaussian, and the spike train is assumed to be poisson. Given this model, and assuming the poisson spike train can be well approximated as an exponential, a convex objective function can be derived. The objective function was numerically optimized given a nonnegativity constraint on the spike train implemented using a barrier term. Parameters were manually determined and not estimated from the data. Once we ran the deconvolution algorithm on all contours with at least a 5% ΔF/F within one movie we stored them in a matrix. Finally, we correlated the vectors, each representing the estimated spike train from a single contour, using the MATLAB built in function CORRCOEF, which calculated correlations according to the following standard formula for computing correlation coeffcients (R):

$$R(i,j) = \frac{C(i,j)}{\sqrt{C(i,i)C(j,j)}}$$

Chapter 3 - Characterization of Inhibitory Subtypes

Introduction

Understanding the order and variability in neocortical inhibitory circuits is one of the most provocative challenges in circuit neuroscience. The neocortex has several subtypes of inhibitory interneurons, all of which have diverse morphological, physiological molecular and synaptic properties (Gupta et al., 2000; Markram et al., 2004). Although most agree that the diversity of neurons within this group confer differential roles within the circuit, the tremendous variation makes functional classification extremely difficult. In fact, to date, there is no consensus as to how many interneuronal subtypes exist, and it remains a current topic of active investigation (Ascoli et al., 2008).

Despite these difficulties, there are a few well agreed-upon criteria for distinguishing one class of interneurons from another. GABAergic synapses cover most of the membrane surface of pyramidal neurons, from the distal dendritic shafts to the cell bodies and the axon initial segments. The synapses in the different domains of pyramidal cells are formed from interneurons of distinct cell types, and therefore the postsynaptic targeting of interneurons (i.e. dendritic targeting versus perisomatic targeting) is commonly used to differentiate them (Karube et al., 2004; Kawaguchi and Kubota, 1997). Even within this basic classification scheme, it remains a challenge to understand whether interneurons targeting different compartments play different functional roles within the neocortical circuit, and how their firing may relate to the activity of surrounding excitatory cells (Freund and Katona, 2007; Miles et al., 1996).

A starting point for studying inhibitory and excitatory neuronal functions is to characterize the firing of these cells during activated states. To do this we used a thalamocortical slice preparation, in which the connections between the thalamus and somatosensory cortex are preserved. Stimulation of the thalamus results in a robust response in cortex, pushing the vast majority of cells in the associated somatosensory cortex to depolarized membrane potentials, and increasing their likelihood to fire action potentials. These UP states, or "ensemble activations" involve multiple cells types, providing a good substrate for comparing neuronal activity patterns among different subclasses. By understanding the activity of cell types under these conditions, we may be able to begin garner insights into their function within the cortical circuit.

In the experiments we performed for this study, we studied the participation of three cell types that are central to neocortical function. Specifically we studied 1) regular spiking (RS) cells, which represent almost excussively pyramidal neurons, 2) parvalbumin (PV) expressing interneurons, which target the perisomatic region of downstream cells and 3) somatostatin (SOM) expressing interneurons which target the dendrites. While synapses from RS cells onto PV interneurons undergo short term synaptic depression in response to incoming spike trains, synapses on to SOM interneurons show strong short term facilitation (Beierlein et al., 2003). This finding is also true thalamic cortical synapses in layer 4, leading to the proposal that PV cells are the main source of inhibition early during a sensory response, and SOM cells provide the majority of late inhibition (Tan et al., 2008).

We targeted each of these 3 cell types for whole cell patch clamp and compared the firing characteristics of these cell types during thalamically- triggered cortical activity. This included

both characterizing how a given cell type responded during each activation, but also how neurons belonging to different cell types fired relative to one another. We found that PV, SOM and RS cells were active during the response, and that the likelihood of any given cell to fire was the same, regardless of cell type. PV and SOM cells that were active, however, tended to fire about twice as many action potentials as RS cells. We found no difference in the time to first spike in the three subtypes. PV and SOM interneurons both tend to fire at higher firing rates than RS cells, and PV cells fired at higher rates than SOM cells. Finally, analysis of the timing to all spikes showed that there were no significant differences in overall timing of each subtype relative to one another. These results suggest that one way inhibitory neurons may compensate for their low numbers is by having higher firing rates than excitatory cells. They also imply that inhibition at the soma and cell body are balanced throughout the length of the response, rather than being differentially recruited, contradictory to what may be predicted by their synaptic properties alone.

Identification and characterization of cell types

In order to identify PV interneurons we made use of a transgenic mouse line in which GFP is expressed in neurons expressing parvalbumin (Chattopadhyaya, 2004). In this mouse line, all GFP cells recorded from (which will be referred to as "pvGFP" cells for the rest of this dissertation) were 'fast spiking' interneurons with marked after-hyperpolarizations, narrow spike widths, and high spike rates (n = 43, Figure 1a, top). These cells did not display significant spike rate adaptation. In addition, pvGFP interneurons had a significantly higher input resistances and

rheobases than other cell types (see Table 1). Morphologically, they resembled basket cells (Figure 1a, bottom).[2]

SOM interneurons, were identified in a separate transgenic mouse line in which neurons expressing SOM are labeled with GFP (Oliva et al., 2000). In this mouse line all GFP cells targeted for intracellular recording were interneurons, as defined by nonpyramidal structure or functional characteristics. Electrophysiologically, SOM GFP ("sGFP" cells for the rest of this dissertation) cells had a marked after hyperpolarization, a moderate frequency of discharge, and significant spike frequency adaptation (n = 50; Figure 1b and Table 1). Morphologically, most sGFP cells were Martinotti cells, with axonal projections toward the pia. These characteristics confirmed that GFP cells were somatostatin positive interneurons (Halabisky et al., 2006; McGarry et al., 2010; Oliva et al., 2000; Wang et al., 2004).

Regular spiking (RS) cells were patched simultaneously with SOM and PV neurons in both transgenic mouse lines. In agreement with previous studies (Feldmeyer et al., 1999), RS cells fired regular trains of single action potentials with low firing rates (n = 62; Figure 1c and Table 1). These cells morphologically resembled either spiny stellate cells or pyramidal cells (a pyramidal cell is depicted in Figure 1c, bottom).

[2]It is worth noting that many of the intrinsic properties of fast spiking interneurons, change as these neurons mature between the ages of p10-p18 (Goldberg, et al 2011). Since we made recordings from p12-p18 animals, the properties we report here should be considered with that in mind.

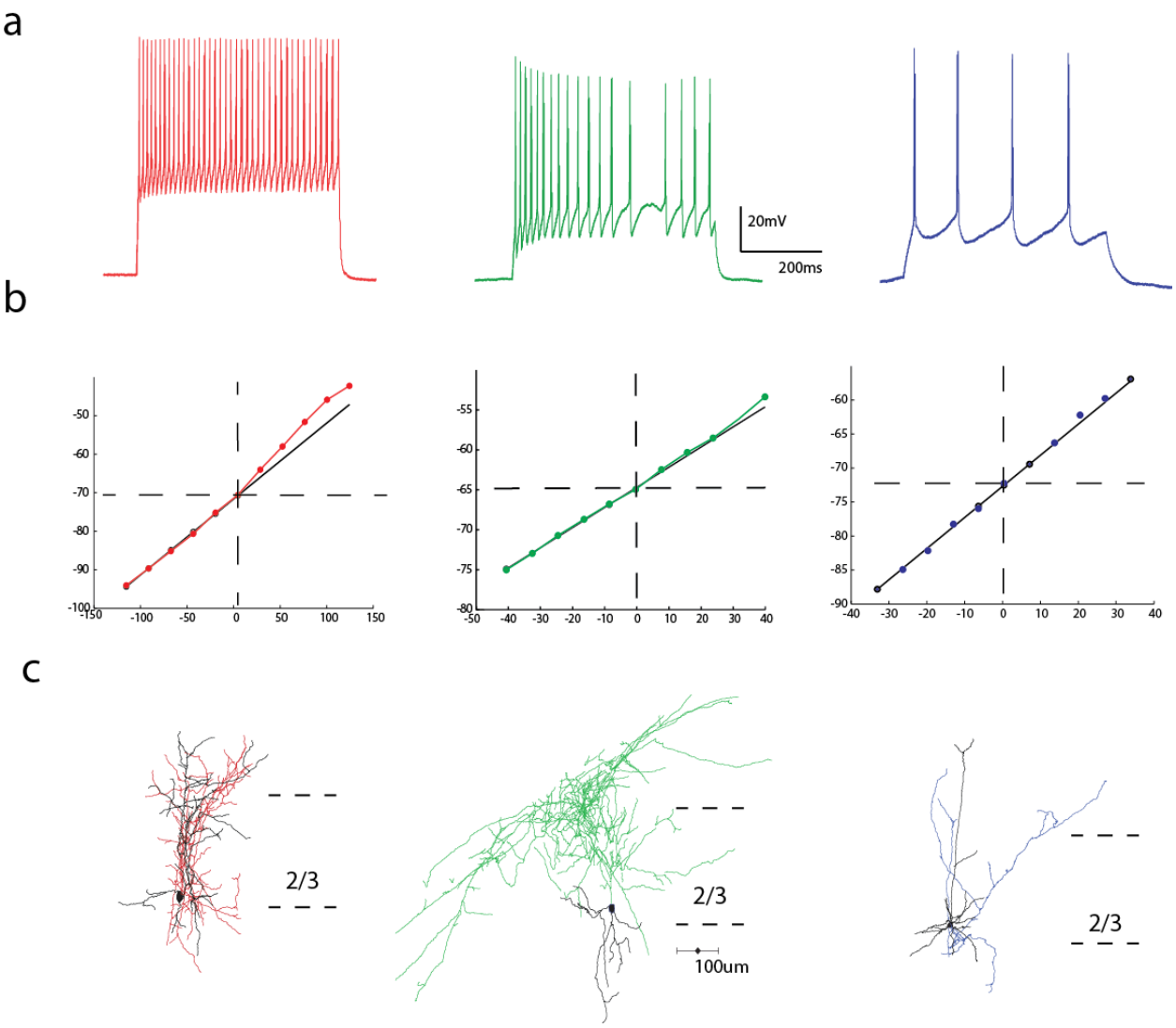

Figure 1. Physiology and anatomy of PV, SOM, and RS cell types

(A) Voltage responses in pvGFP interneuron (left), sGFP interneuron (middle) and RS pyramidal cell (right) to 500ms current injections at twice the rheobase.

(B) IV curves of pvGFP cells of pvGFP, sGFP, and RS neurons. Note the non-linearity of in the pvGFP cell[3], and the linear I-V relationships in sGFP and RS cells.

(C) Reconstructions of a pvGFP basket cell, a sGFP martinotti cell, and a RS pyramidal cell. Dendrites are in black, axons in color, layer boundaries are indicated with dashed lines. Reconstructions are orientated such that the pial surface is at the top.

[3] This IV curve is taken from a p12 pvGFP cell. The properties of these cells change between the ages of p10-18, and this non linearity is reduced dramatically (Goldberg, et al). Nevertheless, this property helped us to confirm we were recording from fast spiking cells in the majority of pvGFP cells we patched.

Table 1. Characteristics of PV, SOM, and RS cells during thalamic activations

	pvGFP	sGFP	RS
Number of cells	42	50	62
Input Resistance (MΩ)	225 ± 29.0	400 ± 88.9	542 ± 76.3
AP half width (ms)	.712 ± 0.07	1.05 ± 0.09	1.65 ± 0.13
Resting membrane potential (mV)	-70.6 ± 1.27	-67.8 ± 0.92	-71.5 ± 0.82
Rheobase (pA)	218.6 ± 31.78	148.4 ± 25.25	51.1 ± 9.15
Firing frequency at 2x threshold (Hz)	65.0 ± 9.04	24.9 ± 3.14	11.0 ± 0.82
Spike Frequency Adaptation	0.79 ± 0.03	0.41 ± 0.04	0.72 ± 0.04

Properties of PV SOM and RS cells during ensemble activations

We set out to determine whether pvGFP, sGFP, and RS cells had differential subthreshold characteristics during thalamically triggered cortical activity. The ventrobasal nucleus of the thalamus was given a high frequency stimulus (6 stimuli, 40Hz) and the resulting activity was measured from 1-3 cells simultaneously, in barrel cortex. This stimulus reliably activated groups

on neurons in layer 4 for a duration that greatly outlasted the stimulus (Figure 2a-b). We have shown previously (MacLean et al., 2005) that stimulation of lower frequency (10-20 HZ) was also occasionally capable of eliciting such ensemble activations, but since the reliability of this type of stimulation from slice to slice and within a slice varies widely, we used 40Hz stimulation for this study.

We first examined membrane potential fluctuation in pvGFP cells, sGFP cells and RS cells during thalamically-triggered ensemble activations. Ensemble activations were automatically detected using an algorithm that required the membrane potential to cross above a certain threshold and stay above that threshold for a minimum amount of time (see Methods). We calculated the average amplitude of the activation in the three cell types. This was accomplished by averaging the membrane potential throughout the activation and subtracting the baseline (see methods). We found that the amplitude of the response was lower in sGFP cells than pvGFP cells (sGFP, 6.45 ± 0.37 mV n = 23; pvGFP, 8.82 ± 0.59, n = 21; RS, 8.11mV ± 0.48 mV n = 41; $p < .05$, one way ANOVA), but that difference was only reached significance between sGFPcells and pvGFP cells (PS vs SOM, $p<.05$; SOM vs RS, $p > .05$; RS vs PV $p > .05$, Turkey-Kramer multiple comparisons test; figure 2c). This was surprising, given that we found no difference in resting membrane potential between pvGFP and sGFP cells, and sGFP cells have higher input resistances than pvGFP cells. We also calculated the duration of the activation, or the amount of time between the automatically detected beginning and end of the event in the three cell types. The duration is not significantly different among pvGFP, sGFP, and RS cells (1.79 ± 0.18 s, PV 1.60 ± 0.20 s SOM, 1.63 ± 0.12 s RS, $p = 0.69$, one-way ANOVA , Figure 2d).

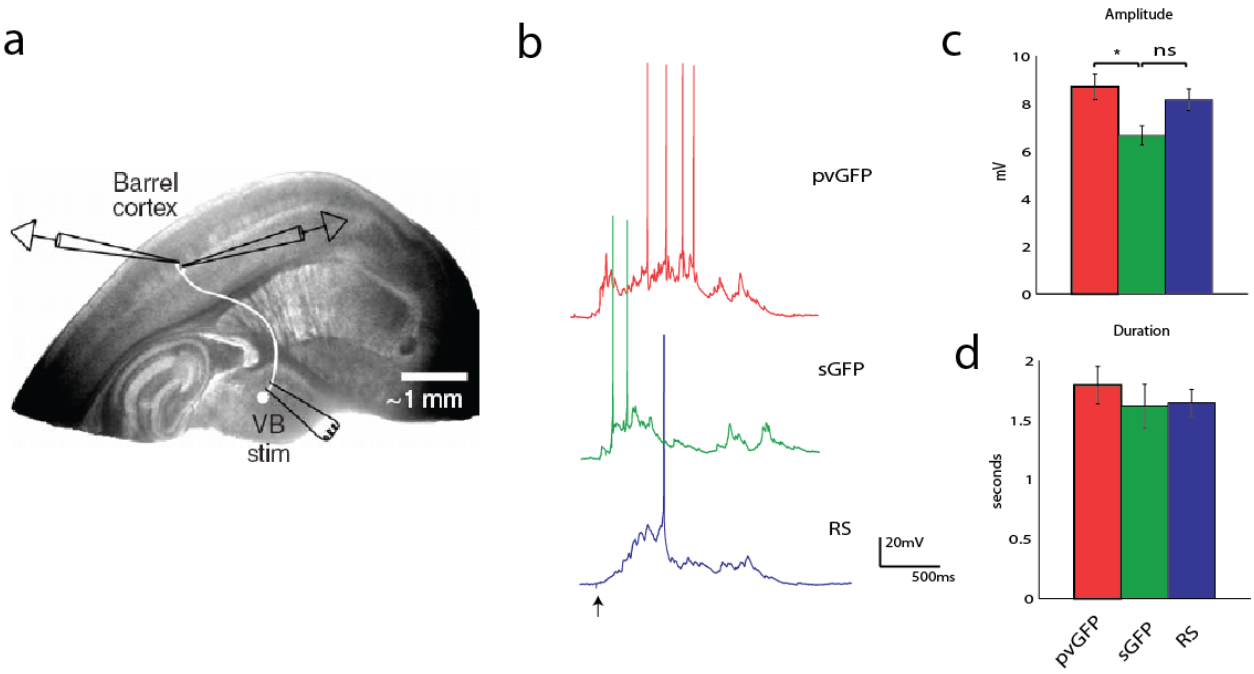

Figure 2. Properties of PV, SOM and RS cells during thalamically triggered activations

(A) Light micrograph, with an overlaid cartoon, of a somatosensory (S1) thalamocortical slice preparation. The ventrobasal (VB) nucleus of the thalamus is where the stimulated electrode (stim) was placed.

(B) Intracellular recordings from a pvGFP interneuron (top), sGFP interneuron (middle), and RS cell (bottom) during a thalamically stimulated cortical activation.

(C) Quantification of amplitude of thalamic response (taken as a mean of the voltage during the entire duration of the activation) in pvGFP (red), sGFP (green) and RS (blue) cell types. Bars represent mean amplitude in each cell, error bars are standard error of the mean (S.E.M.). sGFP cells had amplitudes that were significantly lower than pvGFP cells ($p < .05$,

Turkey-Kramer multiple comparisons test), but not significantly different than from RS cells.

(D) Average duration of the thalamically evoked activation in all three cell types. Bars represent mean duration in each cell, error bars are +/- S.E.M.

Spike timing of RS, PV and SOM cells during ensemble activations

We then inquired whether cells belonging to each of the three cell classes had differential spike timing during ensemble activations. We first asked if there was any difference in the probability that cells belonging to a certain class would fire actions potentials. We found that the percent of cells active in all groups was similar (62% pvGFP, 65% sGFP, and 63% RS, figure 3a). Another important consideration is how reliable cells of each cell class are in firing action potentials. In order to calculate this, for cells which fired action potentials on at least one trial, we calculated the probability of these cells in firing at least 1 action potential on any given trial. Although sGFP cells seemed fire action potentials somewhat more reliably than either pvGFP cells or RS cells to fire action potentials, this difference was not significant when comparing all three groups (PV .66 ± .09, n = 13; SOM .77 ± .06, n = 15; RS .58 ± .05, n = 26; one-way ANOVA $p = .08$, figure 3b). When we compared the groups pairwise, however, we found that SOM cells did fire significantly more reliably than RS cells (Mann-Whitney test, $p < .05$).

We also calculated the total number of action potentials during the response in the three cell types. For this analysis, we excluded cells that never fired action potentials. Among neurons that did fire, pvGFP and sGFP cells were significantly more active during UP states than RS cells, firing ~2-4 times more than their excitatory counterparts (pvGFP, 3.53 ± 0.84 APs/event; sGFP 2.57 ± 0.93 APs/event; RS 1.07 ± 0.19 APs/event, figure 3c, $p < .0002$, Kruskal-Wallis test, pvGFP vs. RS $p< .01$; sGFP vs. RS, $p<.01$, Dunn's multiple comparison test). The difference in number of

APs between pvGFP and sGFP cells was not significantly different ($p > .05$, Dunn's Multiple Comparisons Test).

Next, we asked whether cells belonging to the three cell types are differentially recruited at the start of the response. In order to quantify this, we first calculated the latency to the first spike from the beginning of the activation, or time to first spike. All cell types were capable of firing within ~200ms of activation onset and no significant difference was observed among the cell types. RS cells tended on average to fire significantly later than sGFP and pvGFP interneurons (0.417 ± 0.082 s PV, n = 13, 0.356 ± 0.107 s sGFP, n = 15, .563 ± 0.060 s RS, n = 26 $p < .05$, Kruskall-Wallis test; figure 3d), indicating these cell types are recruited before RS cells at the start of the response. We also compared the distribution of time to all the spikes among the three subtypes relative to the start of the stimulated response. Because the number of total spikes in all groups was different between to three groups (pvGFP, 314; sGFP, 430; RS, 164), we normalized the count of spikes in each time bin from the start of the response to the total number of spikes. Thus, we compared the probability distribution of spikes from time of response onset to the end of the response among the three subtypes (Figure 4a). All three subtypes tended to fire the most approximately 250ms after the start of the response, and taper off steeply after 1 second. sGFP cells firing tended to taper off earlier than either pvGFP cells or RS spiking cells which may suggest somatic inhibition is more important at the termination of the response. However, when comparing the distributions of the three subtypes, we did not detect any significant differences (Friedman test, P = 0.357), implying that overall, the three subtypes do not have distinct times of activation throughout the response.

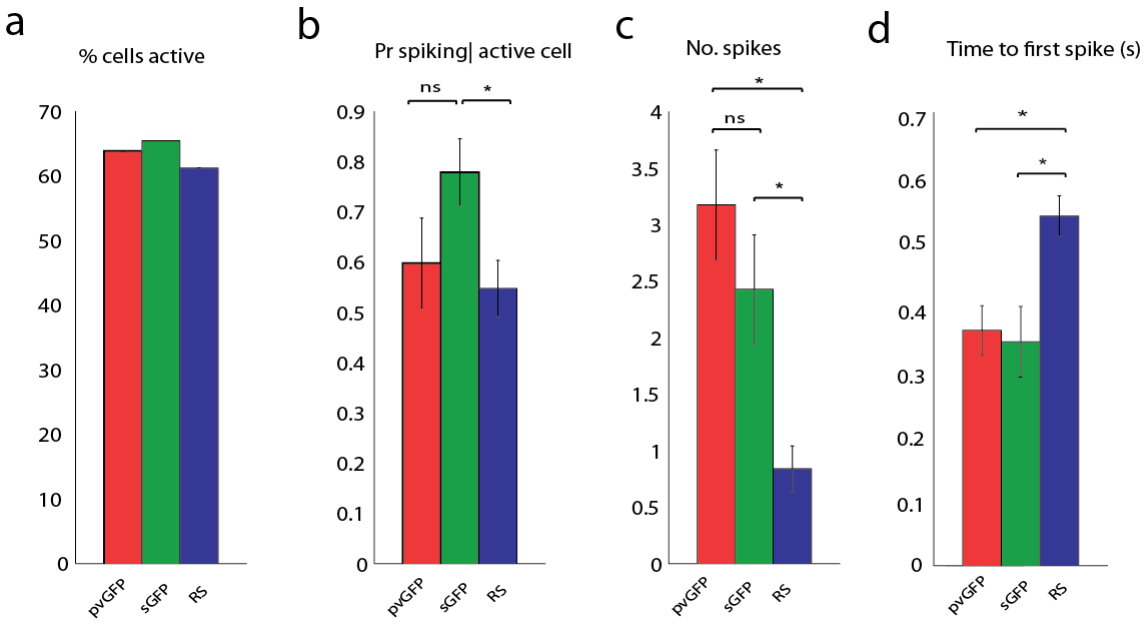

Figure 3. Profiles of active PV, SOM and RS neurons

(A) Percent active of pvGFP interneurons (red), sGFP interneurons (green) and RS cells (blue). The percent represents the proportion of cells in each of the 3 subclasses that fired an action potential in at least one trial in response to thalamic stimulation.

(B) Average probability of spiking in active cells. Each bar represents the probability in any given trial of an active pvGFP, sGFP, or RS cell to spike. Active sGFP cells had a higher probability of spiking than RS cells ($p < .05$, Mann-Whitney test), but not pvGFP cells ($p = .419$, Mann-Whitney test). Probability of spiking was not different between pvGFP cells and RS cells.

(C) Average number of spikes in active cells. Each bar represents the mean number of spikes for a particular subclass. The number of spikes fired by pvGFP and sGFP cells was significantly higher than for RS cells (one way ANOVA with Dunn's multiple comparisons

test, $p < .05$). The difference between number of spikes fired in pvGFP versus sGFP was not significant ($p < .05$ Dunn's multiple comparison test).

(D) Mean time to first (tt1st) spike in active cells. Quantification of the time to the first spike in each subclass. Time to spike was calculated from the automatically detected start of the activation. The tt1st spike was significantly shorter in pvGFP and sGFP cells when compared to RS cells ($p < .05$; Kruskall-Wallis test with Dunn's multiple comparison test).

Finally, we compared the interpike intervals (ISIs), or spike rates, among the three cell classes. Given that pvGFP cells, sGFP cells and RS display different maximal firing rates during somatic current injections (see Table 1 and Figure 1), we were curious to see if this property held true during cortical activations. For this analysis we again normalized by the total number of spikes in each group, and plotted the probability distributions of the spike rates (Figure 4b). As predicted by their intrinsic firing properties, pvGFP cells tended to have the lowest ISIs (mean ISI, 0.0864 ± .007 s), followed by sGFP cells (mean ISI, 0.1607 ± 0.0132 s), and finally by RS cells (mean ISI, 0.3196 ± .0308 s), with significant differences among all three groups (Kruskall –Wallis test, $p<.001$). This finding is in good agreement with a wealth of evidence that pvGFP cells respond to a variety of stimuli with faster spike rates than other cell types. However, the mean spike rates observed in these cell types in response to current injection (pvGFP, 65.0 ± 9.04; sGFP, 24.9 ± 3.14; RS, 11.0 ± 0.82) was much higher than their actual mean firing rates observed in response to thalamic stimulation which ranged from 10-15Hz for pvGFP cells, 5-10 Hz for sGFP cells, and .75-6 Hz for RS cells.

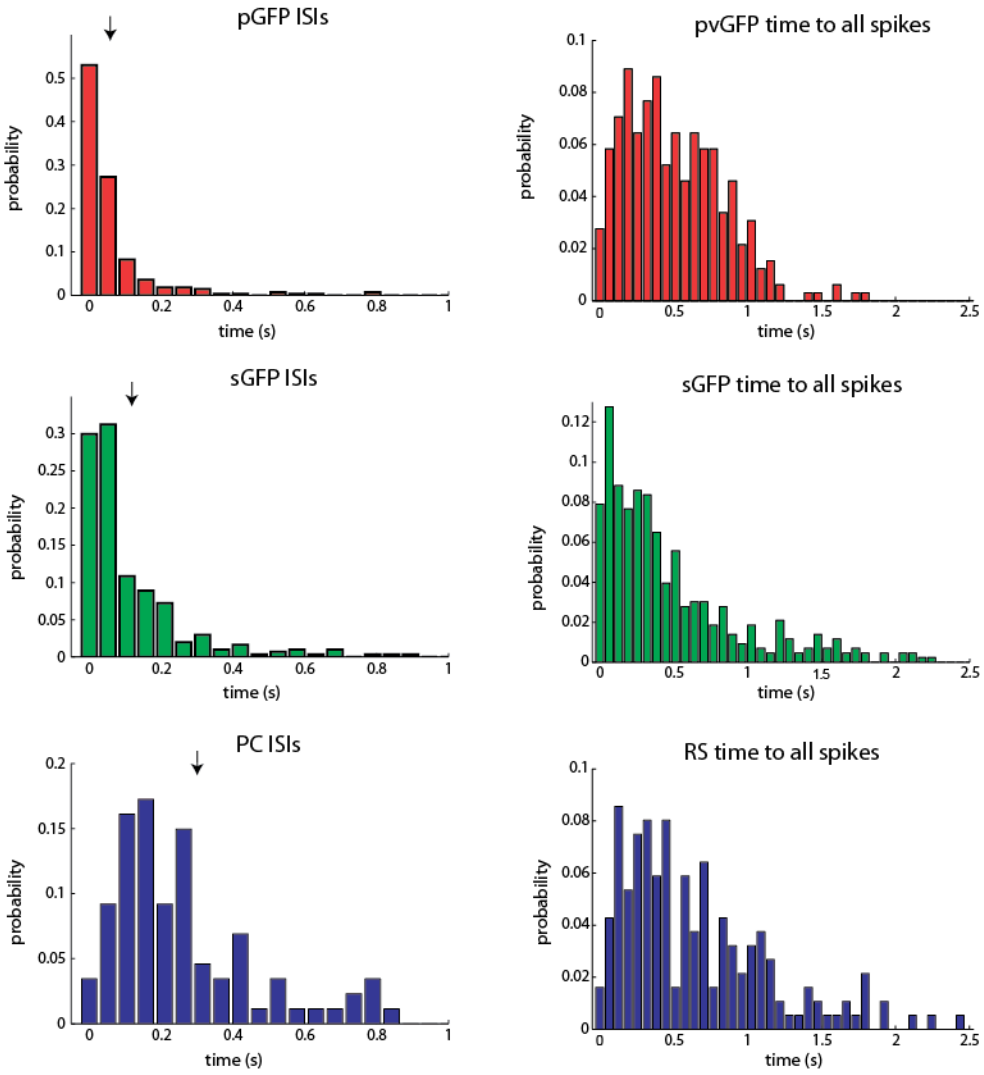

Figure 4. Interspike Interval and timing of all spikes during thalamically stimulated activations

(A) Probability distribution of interspike intervals (ISIs) for pvGFP cells (top, red) sGFP cells (middle, green) and RS cells (bottom). Arrowheads indicate mean ISI for each cell type, significantly different among all three groups (Kruskal-Wallace Test, $p < 0.0001$).

(B) Probability distribution of time to all spikes for the three cell classes, showing the probability of any spike to occur in each time ~65ms bin from the start of the activation. These distributions were not significantly different (Friedman test, $p = 0.357$).

Summary

In this chapter, we recorded simultaneously from either PV cells and RS (pyramidal) cells or SOM and RS cells, and compared their properties during thalamically triggered activations. We found that all three cell types were activated during the activations, and fired readily, with PV and SOM interneurons firing on average 2-4 times more action potentials than RS cells. We found no difference in the time to first spike or the distribution of all spike times among these three cell types, implying that their spikes are equivalently distributed throughout the UP state. Finally, the spike rates of these cells were in good agreement with previous studies and predictions from intracellular current injections; PV interneurons fired at the fastest spike rates, followed by SOM cells and RS cells.

With the properties of each of these cell types during thalamic activations characterized, we next wanted to inquire if 1) the spike timing of neurons within a cell type is more similar than across cell types, which would imply neurons of a given subtype coordinate their outputs to accomplish a given task, and 2) what the function of inhibition is for computations in neocortex. These are the questions addressed in the following two chapters of my thesis.

Chapter 4- Asynchronous Inhibition in Neocortical Microcircuits

Introduction

Information coding in neural networks depends crucially both on the rate of action potential firing (rate code) and the precise timing of spikes (temporal code) across populations of neurons. In addition, this code is not just the property of a single neuron, which by itself has limited capacity to carry information (McClurkin et al., 1991). Instead, the relevant computations to explain perception or behavior must be a property of the simultaneous functioning of many neurons. In sensory cortices, neurons close to each other, within the same layer and cortical column, are likely to receive common inputs, which could result in adjacent neurons processing information in similar ways (Shadlen and Newsome, 1998). Indeed, the spiking activity in neurons within local cortical populations is often correlated (Bach and Kruger, 1986; Gawne and Richmond, 1993; Vaadia et al., 1995; Zohary et al., 1994). Although in some cases correlations may be a fundamental and beneficial component of signal processing (Abbott and Dayan, 1999), a large body of theoretical work demonstrates they can actually impair the estimation of information conveyed by the firing of neural populations, limiting the ability of an organism to make sensory discriminations (Britten et al., 1992; Sompolinsky et al., 2001; Zohary et al., 1994). This may be especially true in cortical areas, such as the barrel cortex, where neurons tend to respond to the same stimulus (Abbott and Dayan, 1999).

Recently, in line with this prediction, a large body of experimental evidence has pointed to an asynchronous coding scheme within sensory cortices. In monkey (Ecker et al., 2010) and

mouse (Smith and Häusser, 2010), it has been found that even when cells have largely overlapping receptive fields, they have remarkably low correlations. Similarly, in rat somatosensory cortex, correlations among neurons close to one another during activated states are also low (Renart et al., 2010).

A major question regarding neuronal coding schemes that has been left largely unanswered in cortex is whether neurons belonging to a particular cell class display correlated firing. This is most likely to be the case among cells that are electrically and/or synaptically coupled, which could allow for synchronization of spikes during any given response. This is especially thought to be the case among interneurons, where cells belonging to the same subtype are commonly electrically coupled (Galarreta and Hestrin, 1999; Gibson et al., 1999; Hestrin and Galarreta, 2005; Tamas et al., 2000), leading to synchronous activity (Blatow et al., 2003; Galarreta et al., 2004; Galarreta and Hestrin, 2001b; Gibson et al., 1999; Merriam et al., 2005) Merriam et al.,2005), and promoting neuronal oscillations (Deans et al., 2001; Gibson et al., 2005; Kaminski et al., 2011). Since most studies focusing on coupling of interneurons examined at most 2 neurons in very close proximity (within 200um), it is unclear how such coupling affects spiking of larger populations within and beyond these distances.

Recent theoretical work has suggested that the ability of electrical coupling to synchronize the activity of cells depends on a number of factors, including coupling strength and firing frequency (Bem et al., 2005; Chow and Kopell, 2000; Di Garbo et al., 2005; Lewis and Rinzel, 2003; Nomura et al., 2003; Pfeuty et al., 2003; Saraga et al., 2006). This theoretical work predicts that, under most conditions, electrical synapses promote synchronous activity, but they can also support antiphase activity between coupled neurons (Vervaeke et al., 2010). Therefore, it is

unclear how such coupling affects interneuronal firing under conditions in which the circuit is active given a relevant stimulus.

In our study, we use fast two photon calcium imaging combined with electrophysiological recordings to study correlations among populations of cells belonging to the same subtype during cortical activations in somatosensory cortex. For this task, we chose a thalamocortical slice preparation in which recurrent cortical activity (UP states) can be thalamically triggered or occur spontaneously. This type of activity occurs in vivo (Luczak et al., 2007; Sanchez-Vives and McCormick, 2000), and the recruited neurons have repeatable spatiotemporal structure, making them a good substrate for studying the firing patterns among cells (Cossart et al., 2003; Luczak et al., 2007; MacLean et al., 2005). We examined parvalbumin- and somatostatin-positive, as neurons with both of these neurochemical markers have been shown to be coupled electrically (Beierlein et al., 2000; Galarreta and Hestrin, 1999, 2001a) and/or chemically (Hu et al., 2011), and together these subtypes make up approximately 80% of all interneurons in the brain. We find, first, that the firing of all neurons is not synchronized, regardless of cell type; inhibitory interneurons, even those that belong to the same class are not more correlated than the general population. Second, paired recordings between neurons of the same type demonstrate that while a small portion of spikes can occur synchronously, overall the spiking of interneurons is not significantly more synchronous than that of pyramidal cells. Finally, we demonstrate that while inhibitory currents are indeed correlated, with inhibition being more correlated than excitation, this is due to a high degree of shared presynaptic input. Taken together, our results provide the first experimental evidence that neurons of the same subtype do not coordinate their activity, providing support for an asynchronous coding scheme in neocortex.

Fast imaging of thalamically evoked activity in interneuron subtypes

To investigate the combined activity of subtypes of neurons, we used thalamocortical somatosensory slices. These slices were bulk loaded with fura-2 AM (Figure 5a) enabling two photon calcium imaging of loaded neurons in layer 4. A spatial light modulator (SLM) was used to split the two photon beam into multiple beamlets, and 40-60 neuron cell bodies were targeted for imaging ((Nikolenko et al., 2008), figure 5a). The SLM obviated the need for raster scanning the excitation beam, allowing us to take advantage of the spatial resolution and high signal to noise ratio two photon imaging affords, while collecting fluorescence at frame rates of 60-66Hz with an EMCCD.

We measured the changes in fluorescence in the cell bodies after giving a brief stimulus train to small areas of ventrobasal thalamus (6 stimuli at 40Hz), which reliably activated groups of neurons in layer 4 barrel cortex (figure 5b). A fast nonnegative deconvolution filter was used to infer the most likely spike train of each neuron given the fluorescence observations (Vogelstein et al., 2010). To calibrate the algorithm, we performed cell-attached patch clamp recordings (n = 11) from neurons identified during the stimulus driven cortical response (Figure 5C). The algorithm performed well at estimating the likelihood of a spike in any given frame, even when we made no allowance for a window of jitter around the time of the actual spike (sensitivity, 80.0 ± 2.5%, specificity, 98.1 ± 0.5%), and detected nearly all spikes within a window of +/- 1 frame (sensitivity 95.0 ± 3.1%, specificity, 95.5 ± 1.4%, figure 5D). With the ability to detect single spikes with such high temporal resolution, we could for the first time address the timing of coordinated activity in subgroups of neurons.

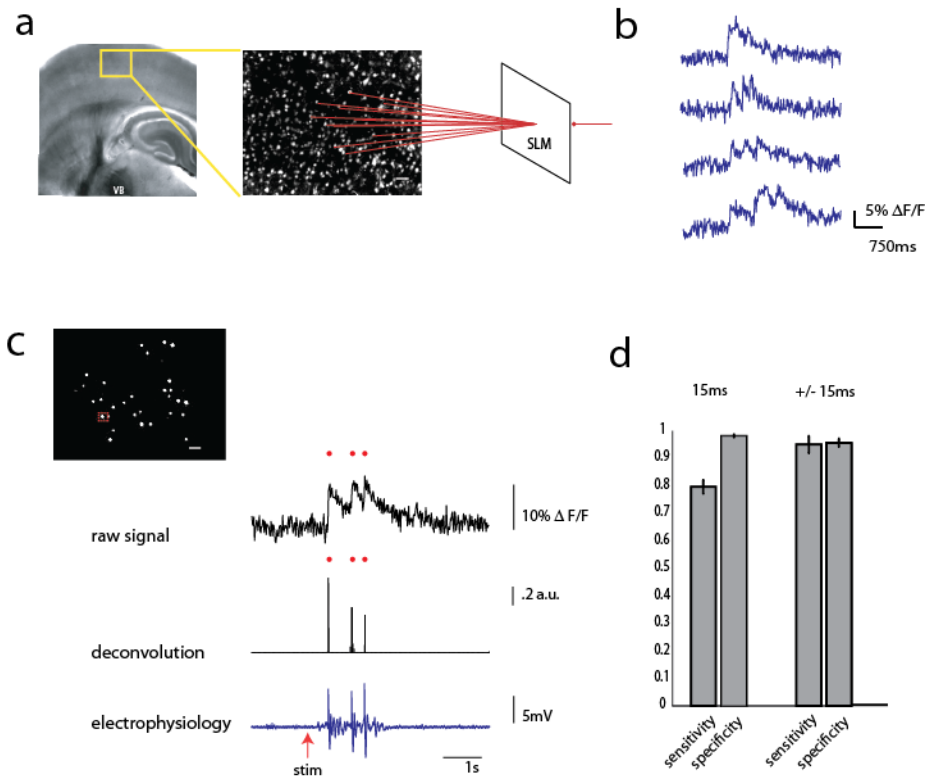

Figure 5. Two photon fast calcium imaging with a single spike deconvolution algorithm

(A) Light micrograph of a somatosensory (S1) thalamocortical slice preparation with intact thalamic input nucleus (ventral basal nucleus, VB), thalamocortical axons and the somatosensory cortex. A stimulating electrode is placed in VB. Superimposed yellow box indicates location, over layer 4, of illustrated two photon z stack to right. Neurons pictured in this field are loaded with fura-2 AM dye, and targeted with a spatial light modulator (SLM, far right) on the cell bodies for continuous two photon illumination during thalamically stimulated activity.

(B) Examples of fluorescence signals showing changes in fluorescence, normalized to baseline (ΔF/F), from four cells illuminated at 790nm on their cell bodies at 790nm with the SLM and imaged at 66Hz With an EMCCD.

(C) Top, left: Two photon image of a single frame showing neuronal cell bodies targeted with two photon illumination with the SLM. Cell outlined in red was targeted in cell-attached mode. Top trace shows raw fluorescence signal from that cell imaged at 66Hz in response to thalamic stimulation. Note that a single spike causes an approximately 5-10% change in $\Delta F/F$. Middle trace is the deconvolution of the calcium signals using parameters obtained from electrophysiology to obtain estimated spike times. Red dots above both traces indicate the time of the actual spikes. Bottom trace shows the associated electrophysiological trace.

(D) Sensitivity (true positive rate) and specificity (1- false positive rate) of the deconvolution algorithm for 11 cells. These rates were calculated while allowing for either no window around each spike to search for a signal, or for a window of +/- 1 frame around each spike. Sensitivity was 80.0 ± 2.5% with no window and 95.0 ± 3.1% with a window of 15ms (1 frame).

Activity of Parvalbumin and Somatostatin subtypes is not correlated

We first performed SLM imaging of GFP labeled parvalbumin (PV) and somatostatin (SOM) GABAergic interneurons to study the timing of activity in these interneurons compared to other cell types (Figure 6a). Experiments were conducted in G42 and GIN transgenic mouse lines, in which PV positive and SOM positive neurons, respectively, are labeled with GFP throughout the cortex (Chattopadhyaya, 2004; Oliva et al., 2000). On average, 35-75% of imaged neurons were "active," or displayed at least a single 5% change in fluorescence, normalized to baseline (ΔF/F), during thalmically triggered UP states. GFP positive PV cells (pvGFP), SOM cells (sGFP) and unlabeled cells ("pvGFP", "sGFP" and "GFPneg" cells, respectively) were found to be active, with no significant differences between these cell types (pvGFP, 53.7 ± 5.4%; sGFP, 68.2 ± 4.6%; GFPneg, 56.4 ± 3.3%; one way ANOVA, $p = .08$, figures 6b-c). Raw signals (ΔF/F) from active pvGFP, sGFP, and GFPneg cells with corresponding spike inference for each trace are shown in Figure 6c. Note that GFPneg cells were imaged alongside labeled cells in both the G42 and GIN transgenic mouse lines.

In order to address the question of whether GABAergic interneurons subpopulations display more correlated firing than other cells types, we computed correlations from the deconvolution spike time estimates, which avoids overestimating the correlation coefficient that results from correlating the raw fluorescence traces themselves (Smith and Häusser, 2010). We computed these correlation coefficients among all pairs of active pvGFP, sGFP, or GFPneg cells during thalamically stimulated UP state. The normalized distributions of the correlations between either pvGFP and GFPneg cells, and sGFP cells and GFPneg cells were similar, showing no

significant differences (Figure 6d; Friedman test, p = .5235). While some cell pairs belonging to all cell types showed correlated activity, in general all groups showed low correlations, with no significant difference between them (correlation among pvGFP neurons, 0.14 ± 0.01 , n = 196 pairs; correlation among sGFP, 0.10 ± .01, n = 67 pairs; correlation among GFPneg cells, 0.12 ± .002, n = 3,119 pairs, from both G42 and GIN animals; p = .4198, Kruskall-Wallis test) Therefore, even when two cells belonged to the same cell class, they did not show similarities in firing when compared to other cell types.

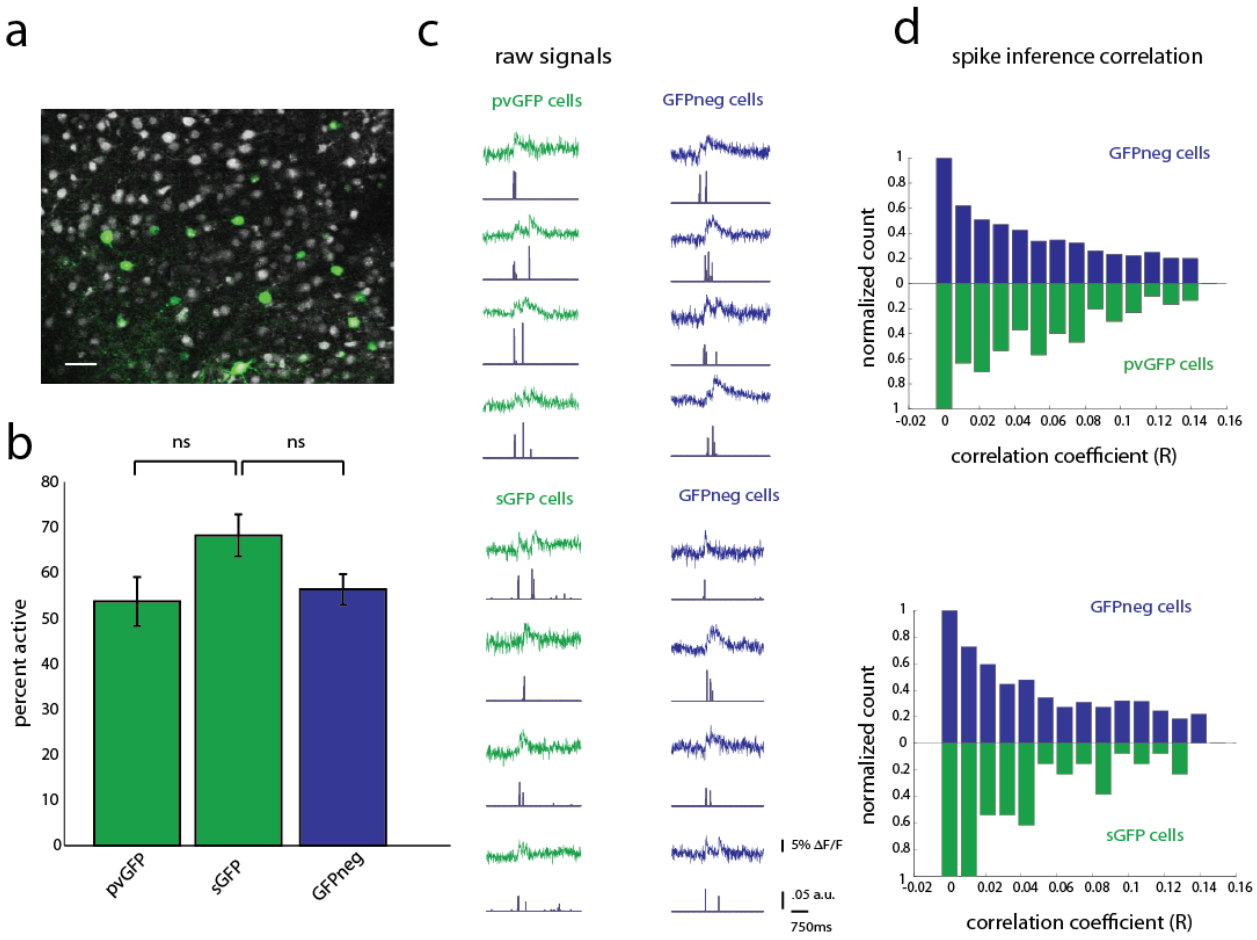

Figure 6. Interneuron subtypes show low correlations during thalamically triggered activity

(A) Two photon image of a loaded slice with labeled interneurons (pvGFP) pseudocolored in green

(B) Quantification of the average percent active pvGFP, sGFP, and GFPneg neurons as determined by SLM imaging and deconvolution. No significant differences were observed across the three groups.

(C) Example fluorescence traces from simultaneously imaged pvGFP and GFPneg cells (top) or sGFP cells and GFPneg cells (bottom) during a thalamically triggered UP state. Spike inference for each trace is shown below each example.

(D) Normalized distribution of correlation coefficients of spike inference for pvGFP interneurons and GFPneg cells (top) and sGFP interneurons and GFPneg cells (bottom). These distributions were not significantly different (Friedman test, $p = .5235$).

Interneuron spiking is not more synchronous than pyramidal cells

Although we found that PV or SOM interneurons did not show correlated activity, we could not exclude the possibility that these neurons were significantly correlated on a time scale faster than the temporal resolution of our SLM imaging (15ms). This seemed especially likely to be the case since neurons belonging to both these subtypes have been shown to be coupled either chemically, and/or electrically via gap junctions, both of which can promote synchrony under certain conditions (Beierlein et al., 2000; Galarreta and Hestrin, 2001b; Hu et al., 2011).

We performed whole-cell electrophysiological recordings from 43 pvGFP interneurons, with biocytin in our internal solution, and performed anatomical and electrophysiological analysis of these cells. Anatomically, these cells resembled basket cells, with densely branching axons, which have been shown to contact the perisomatic regions of postsynaptic targets (Figure 1a). Physiologically, all of these cells were fast spiking interneurons, easily identified by their narrow spike width and large after hyperpolarization potentials (AHPs, Figure 1a). In addition, these cells had high rheobases and fired at high frequencies in response to current injection (see table 1).

We also performed whole-cell electrophysiological recordings from 50 sGFP interneurons. All cells recorded from were interneurons, and were characterized both anatomically and physiologically, in a similar manner as PV cells. Anatomically, the majority of sGFP cells had ascending axon collaterals that branched extensively in layer 1, characteristic of Martinotti cells (Halabisky et al., 2006; McGarry et al., 2010; Wang et al., 2004; Fino and Yuste 2011). Electrophysiologically, in response to current injections, these cells displayed a lower rheobase

than fast spiking cells, and a more moderate frequency of discharge, with significant spike frequency adaptation (see table 1, figure 1b).

To address the question of whether nearby interneurons have synchronous firing patterns, we patched pairs of interneurons within 100um of each other in somatosensory cortex layer 4, where the probability of both chemical and electrical junctions between these cells is high (Figure 7a). We patched 2-4 cells simultaneously to increase the likelihood of observing pairs in which at least 2 interneurons fired action potentials in response to thalamic stimulation. We calculated the time between spikes in every pair of two active cells. In this way, for each spike, we calculated the shortest time between spikes ("minimum inter-cell spike interval") for the two cells patched (Figure 7B). We performed this same analysis for pairs of excitatory principal neurons (PCs) firing action potentials in response to thalamic stimulation. After extracting all minimum inter-cell spike intervals between all pairs of either pvGFP/pvGFP or sGFP/sGFP cells or PC/PC cells, we constructed probability distributions of minimum time between spikes, which show the likelihood of a minimum inter-cell spike interval falling within any given 20ms time bin, from 0 to 1 second (figures 7d-f, middle panels). Surprisingly, the overall minimum spike interval probability distributions were not statistically different between pvGFP, sGFP anPC cells (Friedman test, $p = .6147$), This means that spikes do not occur more synchronously in these two interneuron populations than the general population of principal cells. We also calculated the average minimum time between spikes in all three cell types, and found no significant differences (pvGFP, 219 ± 23.1 ms; sGFP, 191 ± 15.5 ms; PC, 198.12 ± 9.93 ms; Kruskal-Wallis test, $p = .17$). We performed the same calculations for spontaneously occurring activity, and similarly found no difference in either the distribution of minimum spike times (Friedman test, $p = .15$), or the

average minimum spike times (pvGFP, 219 ± 23.1 ms; sGFP, 191 ± 15.5 ms; PC, 198.12 ± 9.93 ms; Kruskal-Wallis test, p = .08; figures 6d-f, far right panels). In order to determine whether or not spiking was more or less synchronous than what would be expected by chance, we reshuffled the spikes, and recalculated the minimum interspike intervals. In all three cells types, PV, SOM and PC we found that no differences in the average minimum spike time intervals between the experimentally acquired data, and the randomly reshuffled data sets (PV, 247.7 ± 19.2 ms, p = .24; SOM, 200.6 ± 14.6 ms, p = .10; PC, 200.6 ± 10.0 ms, p = 0.46, in all cases Mann-Whitney was used and reshuffled distributions were compared to evoked).

We next limited our analysis to pairs of interneurons coupled electrically. Five out of the 12 pvGFP and 4 out of the 11 sGFP pairs were electrically coupled, with coupling coefficients of .031 ± .008 and .085 ± .012, respectively. Among these pairs, we calculated the minimum intercell spike intervals, and compared these to PC in which no cell pairs exhibited electrical coupling. We found that the average intercell spike interval of electrically coupled pvGFP cells and sGFP cells did not differ from that of PC cells (pvGFP cells, 251.7 ± 52.4 ms, p = 0.45 Mann-Whitney; sGFP cells, 200.8 ± 25.4 ms, p = 0.46, Mann-Whitney, in all cases evoked activity in interneurons was compared to evoked activity PC cells). Therefore, electrical coupling does not contribute to synchronous firing in interneurons.

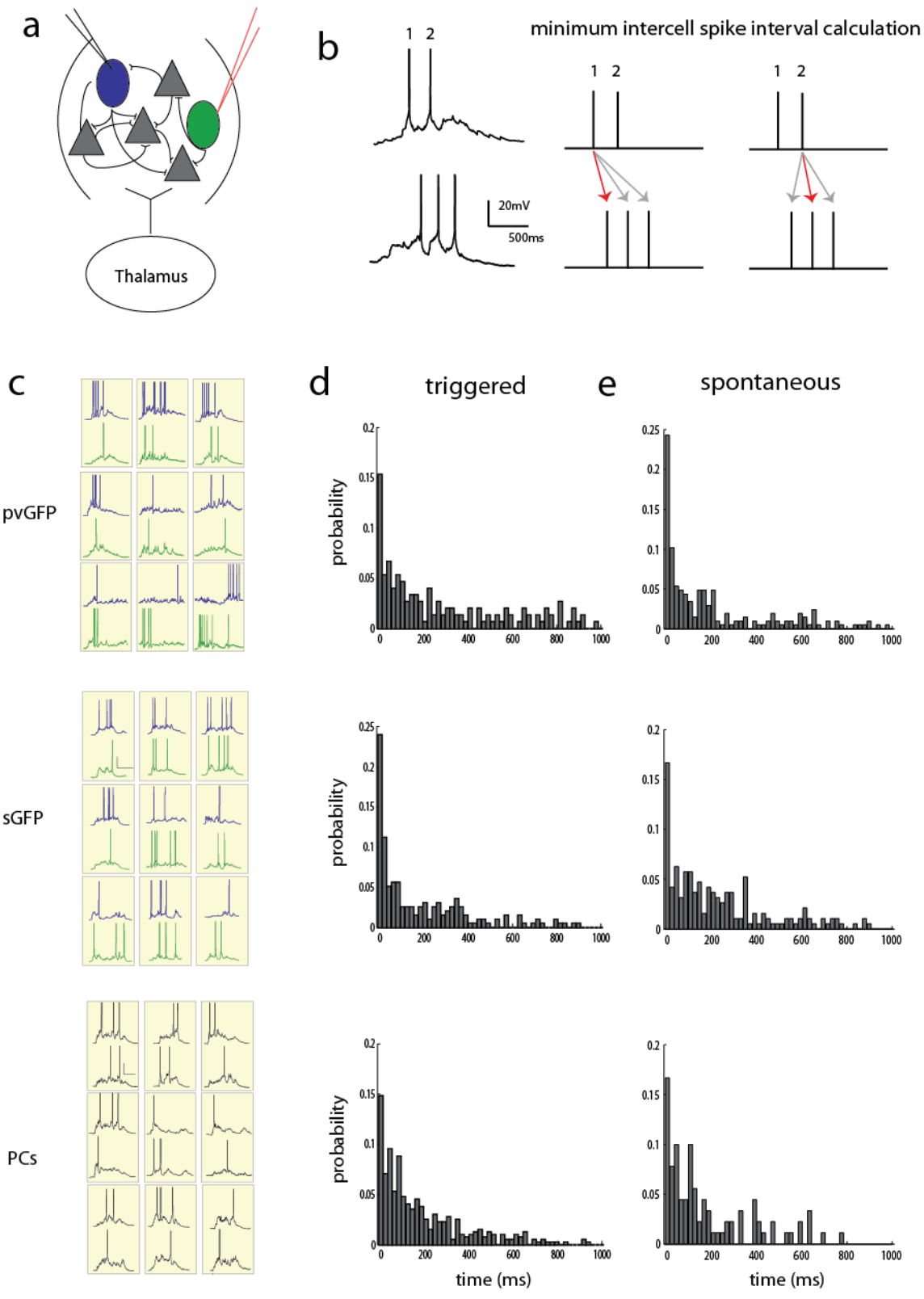
a
Thalamus
b
1 2
minimum intercell spike interval calculation
1 2
1 2
20mV
500ms
c
pvGFP
sGFP
PCs
d
triggered
e
spontaneous
probability
probability
probability
time (ms)
time (ms)

Figure 7. Spiking of interneuron subtypes is not more synchronous than pyramidal cells

(A) Cartoon depicting a layer 4 small recurrent network of cells consisting of interneurons (green and blue) and principal cells (gray). Two nearby cells, either pvGFP, sGFP, or unlabeled principal cells (PC) were patched in whole cells current clamp mode within 200um of one another.

(B) Left, electrophysiological traces from two nearby sGFP cells. To the right, a schematic depicting how the minimum intercell spike interval was calculated for each spike in the top trace to the right.

(C) Far left, representative traces from 9 pairs of simultaneously patched during thalamic stimulation. Top, pvGFP; middle, sGFP; bottom, PCs.

(D) Probability distributions of minimum intercell spike time intervals for pvGFP cells, sGFP cells and PCs during thalamic stimulation

(E) Probability distributions of minimum inter-cell spike time intervals during spontaneously occurring activations.

IPSCs, but not EPSCs, show high correlation during cortical activations

Since we found both in our imaging and electrophysiological studies that interneurons do not seems to exhibit strong synchrony during thalamically evoked or spontaneous activity, we next investigated the timing of inhibitory postsynaptic potentials (IPSCs) compared to excitatory postsynaptic potentials (EPSCs) in nearby PC cells. Such a measurement would be representative of all synaptic inputs and could lend insight into the functional organization of inhibition versus excitation. To this end, we used single-electrode voltage clamp to separate inhibitory postsynaptic potentials (IPSCs) from excitatory postsynaptic potentials (EPSCs). We used an intracellular solution with a chloride reversal of -70mV, allowing us to isolate mostly EPSCs at this potential, while mainly IPSCs were isolated by clamping at 0mV (Figure 8a). Two to four PC cells within 200um were patch clamped, and EPSCs and IPSCs were recorded from these cells on alternate trials, during both triggered and spontaneous activations. IPSCs showed significantly higher correlation than EPSCs in both triggered (EPSCs .55 ± .04; IPSCs, R = .76 ± .04, n = 43 pairs; $p < .001$, Mann-Whitney test, figure8b-c) and spontaneous cortical activity (EPSCs .46 ± .04, IPSCs, R = .66 ± .04 n = 26 pairs; $p < .01$, Mann-Whitney test). Analysis of the cross correlation of EPSCs and IPSCs revealed the half width at half height of the cross correlogram was significantly wider for EPSCs than IPSCs, (156.2 ± 17.1 ms for EPSCs; 68.2 ± 7.49 ms for IPSCs; $p < .001$, Mann-Whitney Test, figure 8d).

Because IPSCs and EPSCs have drastically different rise times, decay times, and amplitudes, it is possible that these parameters could affect the values of correlation obtained by correlating the raw traces. More specifically, the longer decay times typically seen in IPSCs could

increase the correlation value. To address this issue, we detected the times of peaks of both EPSCs and IPSCs, converted these into binary time vectors, and correlated these vectors, using time bins of three different sizes (1, 10, and 100 milliseconds). In this way, instead of correlating the events themselves, which have different characteristics, we correlated only the timing of the events. Even at the smallest time bins analyzed (1ms), the time vectors of IPSCs were significantly more correlated than EPSC time vectors (EPSCs, $R = .037 \pm .02$; IPSCs, $R = .090 \pm .01$ $.p < .001$, unpaired t-test). This was also true at larger time bins we checked, 10ms (EPSCs, $R = .181 \pm .02$; IPSCs, $R = .454 \pm .01$; unpaired t test , $p < .001$), and 100ms (EPSCs, $R = .360 \pm .025$; IPSCs, $R = .695 \pm .027$; unpaired t test , $p < .001$), in both spontaneously occurring and triggered cortical activity (figure 9).

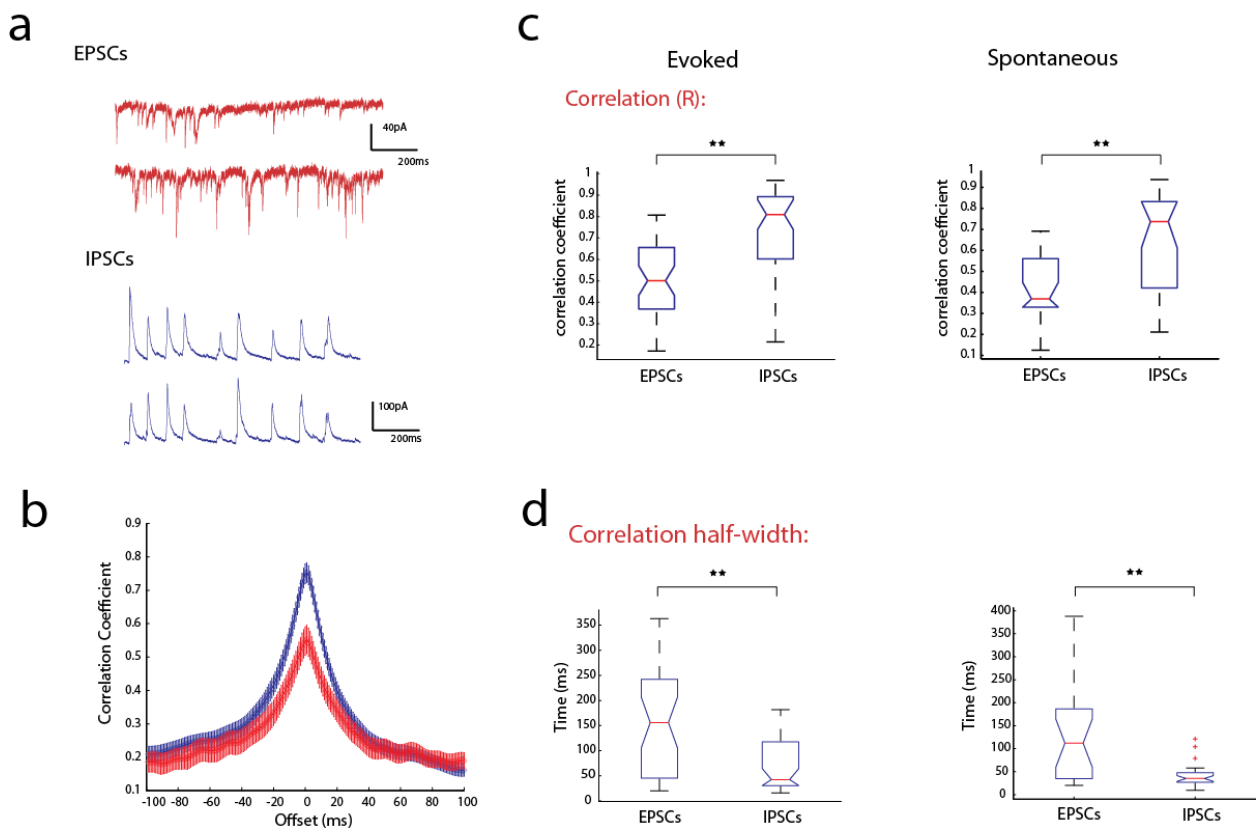

Figure 8. IPSCs are more highly correlated than EPSCs during triggered and spontaneous activations

(A) Recordings from two PCs with cell bodies ~68um apart. Top trace shows EPSCs during thalamic stimulation, bottom shows IPSCs recorded in the same cells on an alternate trial.

(B) Cross correlations between currents at 0mV (blue) and -70mV (red).

(C) Box plots of all correlation coefficients calculated for EPSCs recorded at -70mV and IPSCs recorded at 0mV during evoked activity (left) and spontaneous activity (right). IPSCs were significantly more correlated than EPSCs in both conditions ($p < 0.001$, Mann-Whitney test, n = 43, evoked; n = 26 pairs).

(D) Half width of the cross correlations for EPSCs and IPSCs. The half width is significantly smaller for IPSCs in both conditions ($p < 0.001$, unpaired t test).

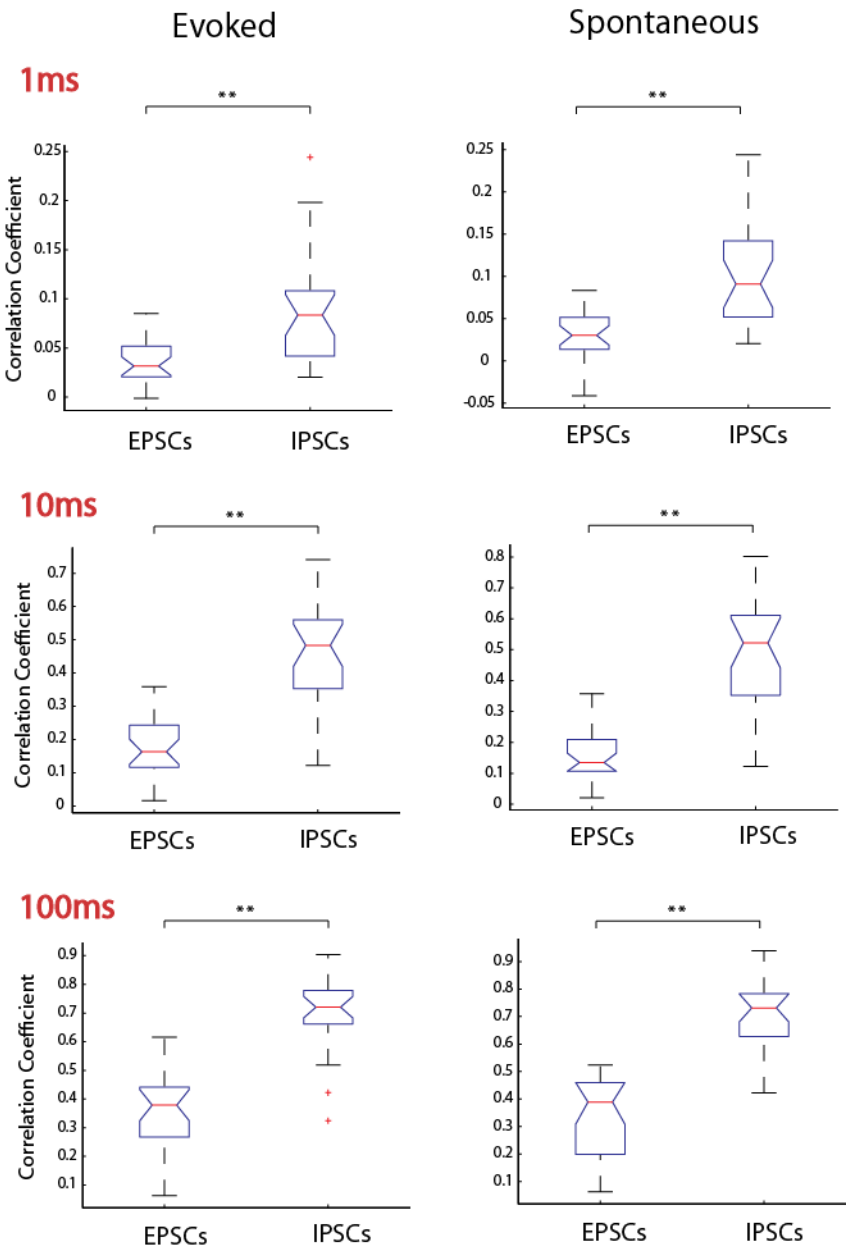

Figure 9. Correlation of Unitary EPSCs and IPSCs confirms IPSCs are more synchronous than EPSCs

Individual IPSCs and EPSCs were detected and, and binary vectors of the event times were constructed. These vectors were then binned in either 1ms (top), 10ms (middle) or 100 ms

(bottom) time bins, and correlated for both evoked and spontaneous activity. Differences in correlation between IPSCs and EPSCs were significant at all time bins, for both evoked and spontaneous activity ($p < .001$, unpaired t test).

Common inhibitory input underlies correlated IPSCs

Two different and possibly overlapping phenomena could explain the synchronous inhibition we found during triggered and spontaneous activity. First, it is possible that interneurons are firing more synchronously than their excitatory counterparts. In this scenario, interneurons would have to fire the majority of their action potentials within the timescale of the increased correlation we found. As illustrated in figure 10a, such synchronization would lead to IPSCs occurring at the same time in nearby pyramidal cells, and could explain the high degree of correlation observed. Second, the higher correlation of IPSCS could be due to shared presynaptic input. In this case, an interneuron would have to be highly connected to downstream pyramidal cells within the distances we checked (30-200um). If this were true, each time an inhibitory interneuron fired an action potential, it would be observed nearly synchronously in all downstream cells (Figure 10a).

Our imaging and electrophysiological experiments led us to believe that perhaps only a small portion of the high correlation we observed in IPSCs could be due to synchronous firing. Therefore, we hypothesized that a high degree of overlapping input from nearby interneurons was primarily responsible for the correlated IPSCs. If correlation of IPSCs is due to shared input rather than synchronous firing, two criteria would need to be met 1) inhibitory connections onto PCs should be much more dense locally than connections from PCs to PCs and 2) each IPSC detected during the thalamic response should be attributable to just one or a few interneurons. In order to investigate this, we performed paired recordings between either pvGFP cells and PCs,

or SOM cells and PCs. We found that within 150um 11/13 (84.6%) of dually patched pvGFP and PC cell pairs were connected. We found a similarly high connection probability between sGFP cells and PC cell pairs (13/17 pairs, or 76.4%) whereas the connection probability between PC pairs was much lower with only 5/39 pairs connected (12.8%). This high probability of connection of interneurons onto PCs fulfills the first criteria (Figure 10b).

Next, in order to get an estimate of how many interneurons contribute to each IPSC during cortical activity, we measured the conductance of each IPSC during triggered activity, and compared these to the conductance of monosynaptic pvGFP→PC and sGFP→PC IPSCs, as measured from paired recordings. The mean conductance of pvGFP→PC connections was significantly higher than that of sGFP→PC connections (pvGFP→PC, 2.08 ± 0.50 nS; sGFP→PC, 0.76 ± 0.24 nS, t test, $p < .05$, n = 11 for pGFP→PC pairs and n = 13 sGFP→PC pairs), which is unsurprising given our recordings were made at the soma, much nearer to where parvalbumin interneurons form synapses onto PCs. More importantly, though, the mean conductances during the cortical activity (1.13 ± 0.02 nS, n = 6578 IPSCS recorded from 15 cells) did not differ significantly ($p = 0.442$, Mann-Whitney) from the combined conductances of PV and SOM inputs (1.36 ± 0.29 nS n = 24, normalized distributions shown in figure 10c). This indicates that each IPSC observed during triggered or spontaneous activity could be made up of just one or at most a few interneurons, fulfilling the second criteria discussed above.

As a final test, we looked at how correlations of IPSCs and EPSCs drop off with distance. Our rationale was that if synchronization was causing the high correlations of IPSCs, the correlations we observed may remain higher over larger distances than would be expected if they were caused by common input. Both IPSCs and EPSCs dropped off rapidly with distance, with

slopes significantly different from zero (EPSCs, n = 30, $p < .001$; IPSCs, n = 25, $p < .001$; linear regression) with no difference in their slopes (analysis of covariance $p = 0.52$, figure 11). The correlations of IPSCs fell off strongly after 100um, which fits very well with the established drop off of the probability of connection for inhibitory connections (Fino and Yuste, 2011; Packer and Yuste, 2011). We conclude that high correlation of IPSCs seen during thalamically driven UP states must be primarily due to shared presynaptic input from inhibitory neurons rather than synchronous firing of interneurons.

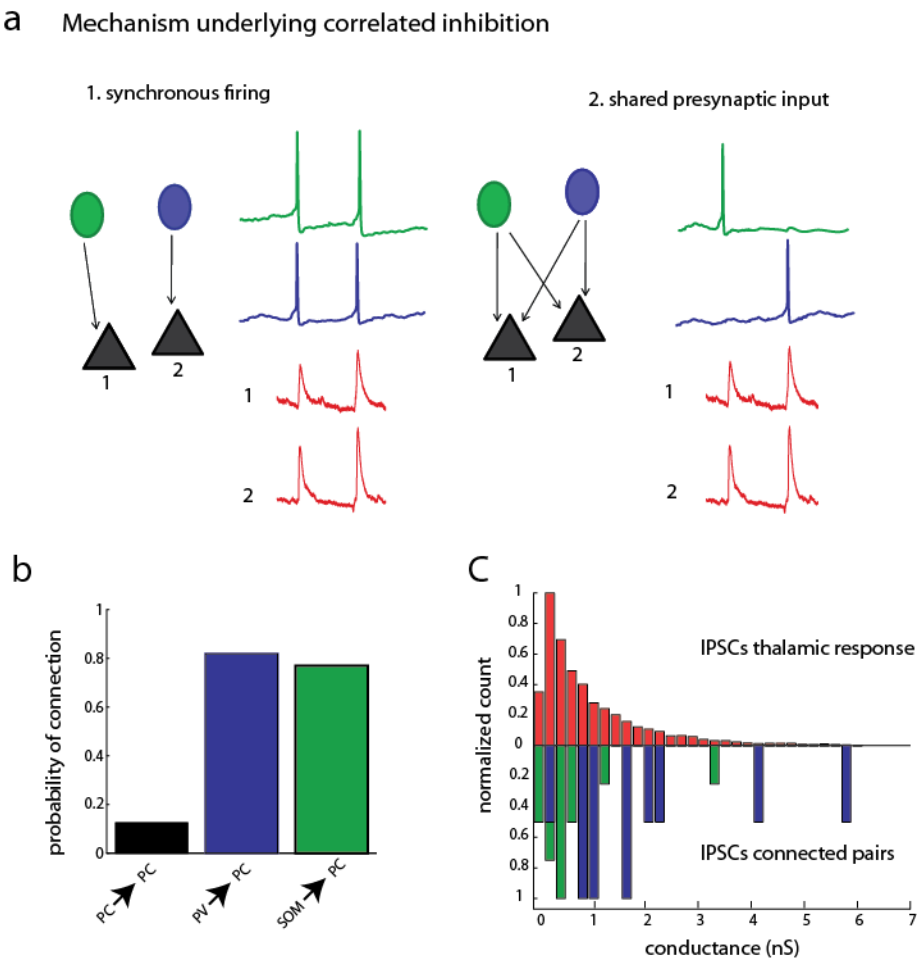

Figure 10. High correlation of IPSCs is due to common input, rather than synchronous firing of interneurons

(A) Schematic depicting two possible mechanisms underlying correlated IPSCs. In the first scenario, depicted to the left, "synchronous firing", correlated IPSCs would be caused by

two or more interneurons firing simultaneously. In this case, each IPSC would be the sum of the spiking of several interneurons. In the second scenario, “shared presynaptic input”, in a system where every interneuron has highly divergent axons and contacts many postsynaptic PCs, each time an interneuron fires a spike, an IPSC would be recorded from all of its downstream postsynaptic targets nearly simultaneously.

(B) Connection probabilities for PC→PC pairs (12,8%), pvGFP→PC pairs (84.6%) and sGFP→PC pairs (76.4%).

(C) Normalized distribution of conductances for IPSCs recorded during thalamically triggered activations (top, red), and synaptic conductances measured from pvGFP→ PC pairs (blue) or sGFP→ PC pairs (green).

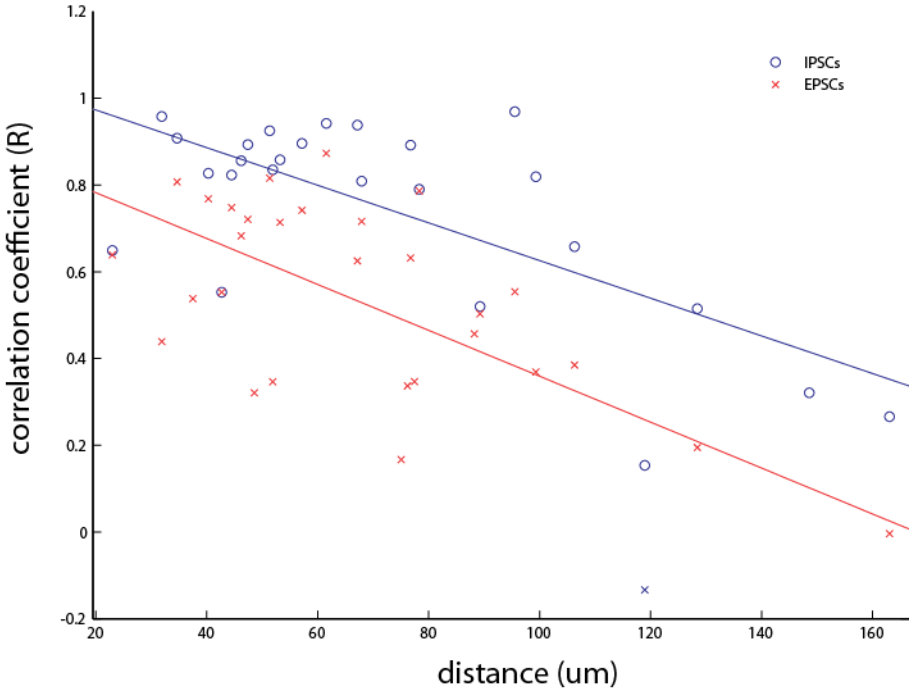

Figure 11. Correlations drop off with increasing distance between cell somas

(A) Correlations of IPSCs (blue) and EPSCs (red) versus distance. Both fall off with distance. Both slopes are significantly different from 0, but not from each other.

Summary

In this study, we used a combination of fast calcium imaging and electrophysiology to study and compare activity in interneurons and excitatory cells. Two-photon imaging with SLMs allowed us, for the first time, to study correlations within two interneuronal subclasses, PV and SOM, respectively, at the population level. We found that neurons exhibit low correlations in response to both thalamic stimulation and during spontaneously occurring UP states. This decorrelated activity was a general feature of all neurons, and surprisingly, neurons within a subclass, specifically PV or SOM interneurons, do not exhibit more correlated firing when compared to the general population. Intracellular recordings confirmed that while some spikes can occur within 10ms of each other in nearby interneurons, the overall distribution of minimum inter-cell spike intervals in interneuronal subtypes and excitatory cells was not significantly different. Finally, voltage clamp recordings demonstrated IPSCs are correlated in cells at close distances, a phenomenon due mostly to shared input rather than synchronous firing. Our data indicate that asynchronous activity is a general feature of all cortical cells, regardless of cell class.

Chapter 5- Discussion

UP States as a model of network activity

UP states are a fascinating model of neurons acting as ensembles. They are clearly coordinated in time and space and thus represent at least one mode of operation in which neurons act as assemblies. Neocortical UP states are a wide spread phenomenon that have been linked to the modulation of global brain states during sleep, quiet wakefulness and sensory processing (Lampl et al., 1999; Petersen et al., 2003b; Shu et al., 2003).

The UP states observed in our preparation resemble endogenous brain activity in several ways. First, UP-states are observed in vivo and are similar to those observed in vitro (Hasenstaub et al., 2005; Luczak et al., 2007; MacLean et al., 2005; Sanchez-Vives and McCormick, 2000). Second, UP-states in vivo and in vitro constitute a high-conductance state, reminiscent of that observed in intact animals (Destexhe and Pare, 1999; Destexhe et al., 2003; Rudolph et al., 2005). Finally, while in most in vitro studies triggering of UP states relies upon using a modified, artificial cerebrospinal fluid (ACSF) containing reduced Ca^{2+} concentration, we used unmodified ACSF, mimicking the situation in vivo more accurately. Therefore we consider the UP-states observed here to be a useful paradigm for studying the normal firing relationships between different types of neurons.

Intrinsic properties of cell types do not predict spiking behavior

The intrinsic properties of the three cell types we studied here varied along several electrophysiological dimensions. These properties, however, do not necessarily predict the neurons' responses during the UP states. PV cells, for example, have low input resistances, which might suggest they are harder to bring to threshold and may fire less during UP states. However, these cells tend to fire more than RS cells, which have significantly lower input resistances. This suggests that synaptic properties, rather than input resistance are most important for determining the frequency with which a cell spikes. In line with this notion, both the probability of connections (Beierlein et al., 2003; Sun et al., 2006) and the synaptic weights of RS cell synapses onto PV cells are higher than for RS cell synapses onto RS cells. Interestingly, SOM cells, which share a high probability of connection from RS cells and have high input resistances, do not spike more than PV cells. In line with this, these cells have significantly lower membrane potentials during the UP state than PV cells, suggesting there may be some other mechanism to equalize the responses in these two cell types. Determining what this is will require further investigation.

Balance of excitation and inhibition

It is generally agreed that in most cortical states and activation schemes, inhibition is balanced with excitation. This is true of recurrent network activity during UP states *in vitro,* which are generated and maintained by a precise balance between excitatory and inhibitory inputs (Sanchez-Vives and McCormick, 2000; Shu et al., 2003). Although this balance seems to be a fundamental principle governing activity in neural circuits, the mechanisms responsible for this balance are not well understood.

Since inhibitory interneurons comprise just 20% of the total population of neurons, in order to balance excitatory neurons, interneurons must either: 1) have higher connectivity rates, 2) have more reliable synapses, 3) have stronger synapses or 4) have higher spike rates than their excitatory counterparts. There is substantial evidence that connection probabilities from GABAergic interneurons onto excitatory cells are higher than excitatory-excitatory connections (Beierlein et al., 2003; Fino and Yuste, 2011; Holmgren et al., 2003; Oswald et al., 2009; Thomson et al., 1996). Likewise, it has been shown that GABAergic synapses transmit signals more faithfully and that they build synapses with higher conductances (Thomson and Deuchars, 1997). Our data confirms the high connectivity and higher strength of inhibitory connections and also suggests that interneurons may also fire more action potentials in order to achieve this balance, as both PV cells and SOM cells fired significantly more than RS cells. This is most likely due to the relatively strong synapses excitatory cells make onto inhibitory neurons, especially of the PV subtype (Beierlein et al., 2003; Bruno and Simons, 2002; Hull et al., 2009; Thomson and Deuchars, 1997).

The short term facilitating dynamics of excitatory synapses onto these cells would suggest that SOM cells may provide this inhibition at later time points than PV cells (Beierlein et al., 2003). However, our data does not support this view. Rather, we found SOM cells and PV cells have similar distributions in their firing time throughout the response, matching the firing of RS cells. Since SOM and PV cells are known to target different compartments of their targets, soma and dendrites, respectively, it may be that inhibition throughout the pyramidal cells is a necessary component of achieving appropriate excitatory/inhibitory balance.

Cell type homogeny among neurons does not confer correlated activity

Two photon imaging, while allowing for good signal to noise, better depth penetration and less bleaching than one photon imaging, has traditionally had a limited temporal resolution. Using the SLM to split the laser beam onto neurons of interest allowed us to achieve an imaging speed of 60Hz using an EMCCD as a wide field detector. This represents a two to five time improvement in speed over standard laser scanning systems. Unlike two photon raster scanning or other techniques[4] the frame rate doesn't scale with the number of cells. Rather, the number of cells that can be imaged with SLM imaging scales with laser power, which has increased substantially in the past few years and will continue to increase. Taking advantage of the high temporal resolution of our data, we employed a deconvolution algorithm that detected spikes with high sensitivity, enabling us to extract spike times in principal cells and interneuron subpopulations. This is the first time, to our knowledge, that correlations among the spiking activity of more than two neurons belonging to a cell class have been reported in an optical assay of network activity.

Intracellular recordings from interneurons with intersomatic distances of less than 150um confirmed that interneurons belonging to the same class did not display more synchronous firing than their excitatory counterparts. This was true regardless of the high incidence of gap junctions found within these distances, indicating that electrical coupling during thalamically stimulated and spontaneous activity does not influence synchrony in PV and SOM interneuron subtypes at fast time scales.

[4] Although scanning speeds have recently been greatly improved by the use of microscopes with resonant scanning mirrors (30 frames per second (fps), acousto-optical defl ectors (AODs; 100s fps) or polygon-mirror scanners. But all of these systems relay on a single excitation beam, and the rate of imaging will decrease with the number of cells and/or field of view imaged.

Our data, demonstrating that neurons belonging to PV and SOM neuronal classes are not more synchronous than simultaneously recorded cells is contradictory to previous evidence indicating that interneurons belonging to both these cell classes can be tightly synchronized, a phenomenon attributed to electrical and chemical coupling between nearby neurons (Hu et al., 2011; Tamas et al., 2000). However, this discrepancy can be explained when one considers that in almost all studies where synchronization has been tested within interneuron subtypes, spiking was induced by introducing current injections in both cells simultaneously, or by activating specific subsets of neurons using neuromodulators . These manipulations do not activate all the conductances relevant during evoked or spontaneous activity in sensory cortex. The interaction of these conductances combined with the electrical and chemical coupling of interneurons is crucial when testing whether this coupling affects synchrony; when neurons are in a high conductance state, it is possible and even likely that gap junction and inhibitory synaptic coupling from nearby cells have a much smaller effect. Therefore, in active cortical circuits where both excitatory and inhibitory neurons are concomitantly activated, electrical coupling among subtypes may be too small compared to the number of synaptic inputs activated, detracting from their ability to synchronize neurons on fast time scales. The main role of gap junctions in active cortical circuits then may be to act as low pass filters, synchronizing subthreshold membrane potentials, and promoting synchrony over broader time scales (Galarreta and Hestrin, 1999, 2001b). Alternatively, gap junctions could play a metabolic role, by enabling cells that belong to the same differentiation program to share second messengers or signaling molecules (Yuste et al., 1992).

Inhibition is dense and nonspecific

In the experiments performed here, we found that when we voltage clamped cells within 100μm at the reversal potentials for inhibition or excitation, isolated EPSCs and IPSCs were highly correlated, with IPSCs much more highly correlated than EPSCs. This result is similar to findings in ferret V1, where the higher degree of correlation among IPSCs in dually patched cells was attributed to synchronization of PV interneurons within the gamma band. However, several lines of evidence lead us to conclude the high correlation we observed in IPSCs is due to a greater degree of shared inhibitory inputs among nearby cells. First, inhibitory neurons, as discussed above, do not fire more synchronously than pyramidal cells. Second, the high probability of finding a connection between parvalbumin-positive and somatostatin-positive interneurons onto pyramidal cells, indicates that shared inhibitory input is likely the main mechanism responsible for IPSC correlation we observed. This finding is in agreement with previous electrophysiological and two photon mapping studies demonstrating both SOM and PV interneuron subtypes make locally dense and unspecific connections. Third, the conductance of each IPSC detected during spontaneous and evoked activity was comparable to the conductance of individual synapses, indicating that the IPSCs during evoked and spontaneous activity could be comprised of just a single interneuron firing, rather than a synchronous group.

Functional implications

So what exactly does inhibition do in cortical circuits? In a variety of brain areas, including hippocampus and cortex, oscillations- representing the collective activity of large neuronal populations and varying in frequency depending on the behavioural state of the animal- are

considered to be important for a variety of higher cognitive functions. Experimental and theoretical studies have shown that interneuron networks are capable of periodically entraining principal neuron firing, providing the substrate for oscillatory behaviour. In addition, it has been shown that the frequency of these oscillations may be determined, at least in part, by the classes of neurons involved; parvalbumin are thought to be important in generating gamma oscillations, while somatostatin interneurons may participate in the generation of lower frequency oscillations (Hasenstaub et al., 2005; Klausberger et al., 2003; Somogyi and Klausberger, 2005). In general, oscillations are thought to synchronize large groups of neurons over great distances, in some cases "binding" one cortical area to another (Singer, 2009). While this certainly may be one function of interneurons in certain behavioral states over *broad* areas of cortex, the data we describe here provide evidence for a different role for interneurons within *local* cortical circuits.

With inhibition itself being asynchronous, it is possible that the primary role of inhibition could be to *desynchronize* rather than synchronize the local network. In both monkey (Ecker et al., 2010) and mouse (Smith and Häusser, 2010) cells display remarkably low correlation even when they are nearby each other and/or have overlapping receptive fields. The mechanisms responsible for this decorrelated coding scheme are the subject of active investigation, but are difficult to elucidate. One reason for this is that exact spike timing in any cell depends on the dynamic interplay of a number of factors including the cell's intrinsic properties and the relative contribution of excitatory and inhibitory inputs. Several network models have proposed that a dynamic balance of excitatory and inhibitory fluctuations counteracts correlations induced by common inputs (Hertz, 2010; Renart et al., 2010). However, direct experimental evidence in support of these models has been scant.

In their theoretical model of decorrelated networks, Renart et al proposed that while isolated EPSCs and IPSCs can be correlated due to common input, these correlations cancel one another, and therefore fall off at intermediate membrane potentials. Indeed the membrane potential correlations we observed by clamping at the reversal potentials for excitation or inhibition dropped off when we clamped at intermediate membrane potentials, suggesting that the interplay between excitation and inhibition is responsible for the desynchronized spiking we observed across neurons (Figure 12). Furthermore, blocking inhibition with gabazine (SR-95531) increased correlations of EPSCs (at -70mV, Figure 13). These experiments lead us to infer that it is indeed possible that a dynamic balance of excitatory and inhibitory fluctuations that counteract the correlations induced by common input. By preventing uncontrolled network-wide synchrony, this mechanism generates a background of weakly- correlated spiking, as required for efficient information processing based on either firing rates or coordinated spike timing patterns (Vogels and Abbott, 2009).

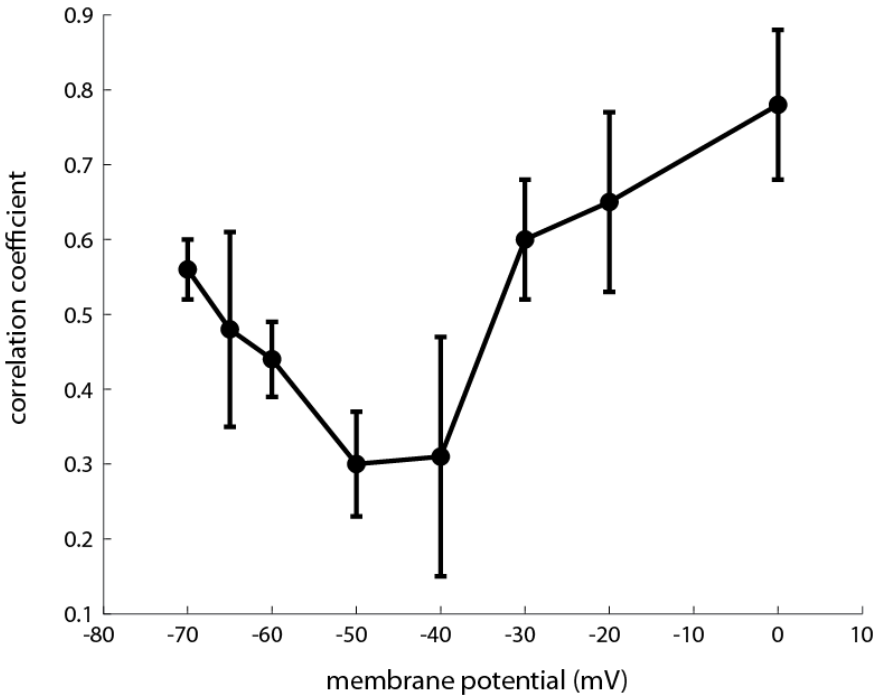

Figure 12. Correlations are reduced at membrane potentials between EPSC and IPSC reversal

Correlation coefficients were calculated for membrane potentials from 0 to -70mV. Correlation was highest at 0mV and -70mV, and lowest at membrane potentials in between these, suggesting IPSC and EPSC correlations cancel one another.

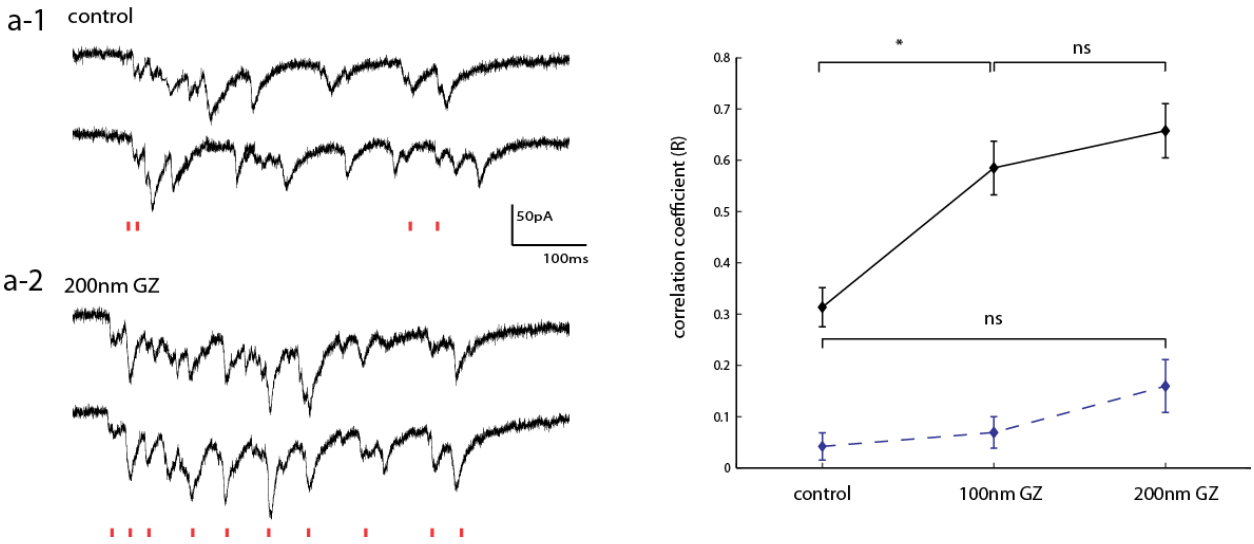

Figure 13. Inhibitory activity decorrelates excitation

(a) Example traces from two PCs recorded ~55 µm from one another. The cells were voltage clamped at -70 mV so that mostly EPSCs were recorded. Above traces are control, and below in 200nm gabazine (GZ). Red lines below each set of traces indicated EPSCs in both cells that occurred within 10ms of one another.

(b) Nanomolar concentrations GZ, increased correlations in EPSCs, and this effect was significant at a concentration of 100nm ($p < .05$, Mann-Whitney, $n = 5$ pairs). Dashed line shows correlation of shuffled data, which did not significantly between control and 200nm GZ (Mann-Whitney, $p = 0.20$).

The decorrelated state of neocortex offers a substantial advantage for information processing: the number of neurons needed to encode a particular stimulus with the same accuracy increases dramatically with increased spiking correlations. This could enable networks of pyramidal neurons to fire at different frequencies regimes without saturating their postsynaptic targets. From this viewpoint, interneurons, by decorrelating the pyramidal cells and spreading their activity over a longer integrating window, could help to stretch the dynamic range of the circuit. In light of our data, it seems plausible that inhibition prevents uncontrolled network wide synchrony, thus providing a general and nonspecific mechanism for decorrelation of local neuronal circuits, and increasing the efficiency of neural coding.

Work in progress and future directions

The experiments I am currently working on, and those I propose for the future focus mostly on two main areas: (1) expanding on the role of inhibition in local microcircuits, and (2) establishing the differential functions of somatic versus dendritic inhibition.

The majority of work presented in this thesis only begins to scrape the surface of the effects of inhibition in cortical microcircuits. While blocking inhibitory signaling pharmacologically is a useful experiment, it suffers from two major problems: (1) it does not allow for good spatial control of blockade of inhibition, and (2) it is not rapidly reversible, making comparisons of before and after the manipulation difficult. Fortunately, with the advent and rapid development of new tools such as optogenetics, allowing for gain or loss of function within specific cell classes, both of these limitations can be overcome. Optogenetics is the combination of genetic and optical methods to control specific events in targeted cells of living tissue, with the temporal precision (millisecond-timescale) needed to keep pace with functioning intact biological systems (Zhang et al., 2010). More specifically, halorhodopsin (NpHR)- the light driven chloride pump that is isolated from singe celled *archaea* organisms- can be employed to inhibit neurons in a subtype specific manner (Zhang et al., 2007).

In a series of preliminary experiments, we took advantage of the most commonly used strategy to date for the expression of NpHR in brain tissue, viral transduction. Viral vectors driving expression of NpHR fused to yellow fluorescent protein (YFP) can be delivered directly into specific brain regions with robust transduction efficacy and limited tissue damage. Using a Cre-loxp expression system (Branda and Dymecki, 2004), the virus was expressed in solely PV

expressing neurons.[5] Immunological co-stainings against PV and YFP demonstrated cell-type specific expression was achieved (Figure 14a). Furthermore, recordings from YFP expressing neurons in acute somatosensory slices confirmed that these cells were indeed typical fast spiking basket cells (Figure 14b, left). Exposing these neurons to light with a wavelength of 550-610nm resulted in robust inhibitory currents (500-1000pA), that were rapidly reversible upon termination of the light source (Figure e 14b, middle). This hyperpolarizing current was enough to stop action potentials induced by current injection at the cell bodies (Figure 14b, right).

With cell type specific expression achieved, we wanted to confirm that inhibitory activity could indeed be reduced during a simple electrical stimulus, while simultaneously measuring the effect of this reduced of inhibition on nearby cells. For this purpose, we used stimulation of the white matter and measured the resulting response in two nearby cells in layer 5. Six stimuli were given to the white matter at frequencies of 10, 20 and 40Hz, and the response was measured in two cells, one in current clamp, the other in voltage clamp. In this way, the magnitude of the response was measured by calculating the amplitude of the EPSP in one cell, while the IPSCs could be simultaneously monitored in the voltage clamped cell (Figure 15a), with and without light activation of NpHR. We found that when we shone light of the appropriate wavelength during stimulation the response was larger, often accompanied by an increase in number of action potentials in the cell from which we recorded EPSPs (Figure 15b).

[5] The Cre-loxp expression system is commonly used to for targeted expression of genes to specific cell types. We used AAV5 DIO-NpHR-YFP knock-in and transgenic Parvalbumin Cre (PV/Cre) mice (Arber, et al) to target the expression of ChR2 to defined neuronal populations. In AAV DIO NpHR-YFP, two incompatible loxP variants flank an inverted version of NpHR fused to the fluorescent marker YFP. In the presence of Cre, a stochastic recombination of either loxP variant takes place, resulting in the inversion of NpHR-YFP into the sense direction, followed by expression of the light-activated channels (Cardin, J.A., Carlen, M., Meletis, K., Knoblich, U., Zhang, F., Deisseroth, K., Tsai, L.H., and Moore, C.I. (2009). Driving fast-spiking cells induces gamma rhythm and controls sensory responses. Nature *459*, 663-667.)

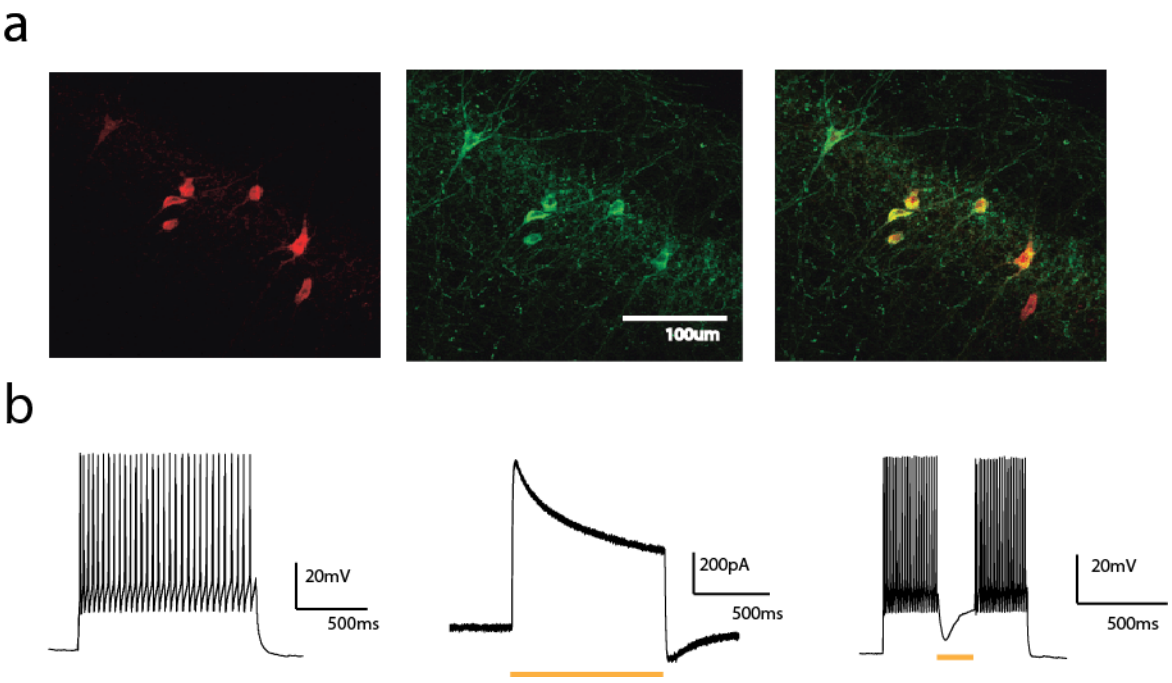

Figure 14. NpHR rapidly and reversibly inhibits PV interneurons

(A) PV^+ interneurons (red, left panel) express YFP (middle panel) 33 d after injection of AAV DIO NpHR-YFP into the barrel cortex of an adult PV-Cre mouse. Right panel shows overlay of PV and YFP expression.

(B) Left: Intracellular recordings from YFP+ cells confirm that these cells are fast spiking basket cells. Middle: inhibitory current measured in a YFP+ cell. Left: 550-610nm light effectively blocks spiking in a YFP+ cell in response to current injection 3x rheobase. Yellow line indicates the duration of the light pulse.

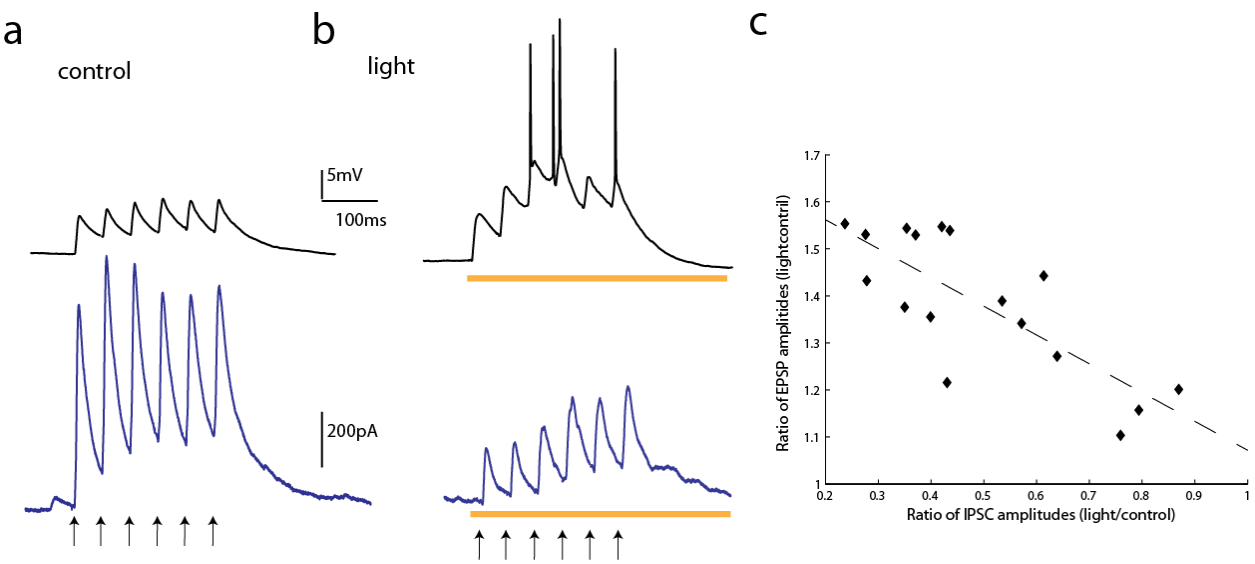

Figure 15. PV interneurons expressing NpHR are effectively turned off during stimulation of afferent pathways

(A) Top, current clamp traces showing EPSPs in response to stimulation of the white matter at 20Hz in control (left) and with light (right); traces are the average of 5 trials. Bottom, IPSCs recorded in an adjacent cell.

(B) Plot of the ratio IPSC amplitudes (light/control) versus the amplitude of EPSP ratios (light/contol). R = .65, indicating a good correlation of IPSC reduction and EPSP enhancement.

This was accompanied by a large reduction in the IPSC amplitude, recorded in the other nearby cell (Figure 15b). We measured the ratio EPSPs with and without light (amplitude of $EPSP_{light}$ /amplitude of $EPSP_{control}$), and compared this to the ratio of IPSCs with and without light (amplitude $IPSC_{light}$ /amplitude $IPSC_{control}$), and observed a linear relationship, implying that the magnitude of the effect we observed was directly proportional to how much inhibition we prevented using NpHR (figure 15c). These preliminary experiments confirm that our expression of NpHR is 1) specific to PV interneurons and 2) effectively blocks activity of these cells during response to stimulation.

Now that we have established this technique, the next step will be to use NpHR to rapidly and reversibly inhibit PV interneurons during cortical UP states. Then, by using either electrophysiology and/or imaging, we could assess correlations of nearby cells during the periods of time we inhibited these neurons. We could alter the timing of our manipulations to try to understand if these interneurons play differential roles throughout the UP state. Finally, using the SLM, we could spatially restrict our light spot to inactivate fewer PV interneurons, and begin to understand the spatial dimensions of inhibition in different areas and layers of cortex.

Perhaps the most important and exciting advantage of using optogeneticsis the ability to express the opsins of interest in a cell type specific manner. We have already expressed NpHR in PV cells, which will allow us to determine the role of inhibition targeting mainly the soma. There also exists a transgenic mouse line which would allow for expression of NpHR in SOM cells. This would enable us to assess the role of these two types inhibitory cells during cortical UP states, and get us much closer to finally understanding if and/or how somatic and dendritic integration

operate to control the output of their downstream targets. Such insights into the distinct roles subtypes of neurons will be invaluable as we continue to try to understand the basic computations performed by cortical microcircuits.

Bibliography

Abbott, L.F., and Dayan, P. (1999). The effect of correlated variability on the accuracy of a population code. Neural Comput *11*, 91-101.

Adrian, E.D. (1914). The all-or-none principle in nerve. The Journal of physiology *47*, 460-474.

Adrian, E.D. (1941). Afferent discharges to the cerebral cortex from peripheral sense organs. The Journal of physiology *100*, 159-191.

Agmon, A., and Connors, B.W. (1991). Thalamocortical responses of mouse somatosensory (barrel) cortex in vitro. Neuroscience *41*, 365-379.

Arieli, A., Sterkin, A., Grinvald, A., and Aertsen, A. (1996). Dynamics of ongoing activity: explanation of the large variability in evoked cortical responses. Science *273*, 1868-1871.

Ascoli, G.A., Alonso-Nanclares, L., Anderson, S.A., Barrionuevo, G., Benavides-Piccione, R., Burkhalter, A., Buzsaki, G., Cauli, B., Defelipe, J., Fairen, A., *et al.* (2008). Petilla terminology: nomenclature of features of GABAergic interneurons of the cerebral cortex. Nat Rev Neurosci *9*, 557-568.

Bach, M., and Kruger, J. (1986). Correlated neuronal variability in monkey visual cortex revealed by a multi-microelectrode. Exp Brain Res *61*, 451-456.

Beierlein, M., Gibson, J.R., and Connors, B.W. (2000). A network of electrically coupled interneurons drives synchronized inhibition in neocortex. Nat Neurosci *3*, 904-910.

Beierlein, M., Gibson, J.R., and Connors, B.W. (2003). Two dynamically distinct inhibitory networks in layer 4 of the neocortex. J Neurophysiol *90*, 2987-3000.

Bem, T., Le Feuvre, Y., Rinzel, J., and Meyrand, P. (2005). Electrical coupling induces bistability of rhythms in networks of inhibitory spiking neurons. Eur J Neurosci *22*, 2661-2668.

Blatow, M., Rozov, A., Katona, I., Hormuzdi, S.G., Meyer, A.H., Whittington, M.A., Caputi, A., and Monyer, H. (2003). A novel network of multipolar bursting interneurons generates theta frequency oscillations in neocortex. Neuron *38*, 805-817.

Branda, C.S., and Dymecki, S.M. (2004). Talking about a revolution: The impact of site-specific recombinases on genetic analyses in mice. Dev Cell *6*, 7-28.

Britten, K.H., Shadlen, M.N., Newsome, W.T., and Movshon, J.A. (1992). The analysis of visual motion: a comparison of neuronal and psychophysical performance. J Neurosci *12*, 4745-4765.

Broca, P.P. (1861). Perte de la Parole, Ramollissement Chronique et Destruction Partielle du Lobe Antérieur Gauche du Cerveau. Bulletin de la Société Anthropologique *2*, 235-238.

Brock, L.G., Coombs, J.S., and Eccles, J.C. (1952). The nature of the monosynaptic excitatory and inhibitory processes in the spinal cord. Proceedings of the Royal Society of London Series B, Containing papers of a Biological character *140*, 170-176.

Brodmann, K. (1999). Brodmann's "Localisation in the cerebral cortex" (London, Imperial College Press).

Bruno, R.M., and Simons, D.J. (2002). Feedforward mechanisms of excitatory and inhibitory cortical receptive fields. J Neurosci *22*, 10966-10975.

Buhl, E.H., Halasy, K., and Somogyi, P. (1994). Diverse sources of hippocampal unitary inhibitory postsynaptic potentials and the number of synaptic release sites. Nature *368*, 823-828.

Buzsaki, G., and Draguhn, A. (2004). Neuronal oscillations in cortical networks. Science *304*, 1926-1929.

Cardin, J.A., Carlen, M., Meletis, K., Knoblich, U., Zhang, F., Deisseroth, K., Tsai, L.H., and Moore, C.I. (2009). Driving fast-spiking cells induces gamma rhythm and controls sensory responses. Nature *459*, 663-667.

Chattopadhyaya, B. (2004). Experience and Activity-Dependent Maturation of Perisomatic GABAergic Innervation in Primary Visual Cortex during a Postnatal Critical Period. Journal of Neuroscience *24*, 9598-9611.

Chow, C.C., and Kopell, N. (2000). Dynamics of spiking neurons with electrical coupling. Neural Comput *12*, 1643-1678.

Cobb, S.R., Buhl, E.H., Halasy, K., Paulsen, O., and Somogyi, P. (1995). Synchronization of neuronal activity in hippocampus by individual GABAergic interneurons. Nature *378*, 75-78.

Coombs, J.S., Eccles, J.C., and Fatt, P. (1955). Excitatory synaptic action in motoneurones. The Journal of physiology *130*, 374-395.

Cossart, R., Aronov, D., and Yuste, R. (2003). Attractor dynamics of network UP states in the neocortex. Nature *423*, 283-288.

Damasio, A.R. (1994). Descartes' error : emotion, reason, and the human brain (New York, Putnam).

Deans, M.R., Gibson, J.R., Sellitto, C., Connors, B.W., and Paul, D.L. (2001). Synchronous activity of inhibitory networks in neocortex requires electrical synapses containing connexin36. Neuron *31*, 477-485.

Del Castillo, J., and Katz, B. (1954). Quantal components of the end-plate potential. The Journal of physiology *124*, 560-573.

Del Castillo, J., and Katz, B. (1955). On the localization of acetylcholine receptors. The Journal of physiology *128*, 157-181.

Destexhe, A., and Pare, D. (1999). Impact of network activity on the integrative properties of neocortical pyramidal neurons in vivo. J Neurophysiol *81*, 1531-1547.

Destexhe, A., Rudolph, M., and Pare, D. (2003). The high-conductance state of neocortical neurons in vivo. Nat Rev Neurosci *4*, 739-751.

Di Garbo, A., Panarese, A., and Chillemi, S. (2005). Gap junctions promote synchronous activities in a network of inhibitory interneurons. Biosystems *79*, 91-99.

Diamon, J., and Yasargil, G.M. (1969). Synaptic function in the fish spinal cord: dendritic integration. Progress in brain research *31*, 201-209.

Duzel, E., Penny, W.D., and Burgess, N. (2010). Brain oscillations and memory. Curr Opin Neurobiol *20*, 143-149.

Ecker, A.S., Berens, P., Keliris, G.A., Bethge, M., Logothetis, N.K., and Tolias, A.S. (2010). Decorrelated Neuronal Firing in Cortical Microcircuits. Science *327*, 584-587.

Fatt, P., and Katz, B. (1952). Spontaneous subthreshold activity at motor nerve endings. The Journal of physiology *117*, 109-128.

Feldmeyer, D., Egger, V., Lubke, J., and Sakmann, B. (1999). Reliable synaptic connections between pairs of excitatory layer 4 neurones within a single 'barrel' of developing rat somatosensory cortex. The Journal of physiology *521 Pt 1*, 169-190.

Feldmeyer, D., Lubke, J., Silver, R.A., and Sakmann, B. (2002). Synaptic connections between layer 4 spiny neurone-layer 2/3 pyramidal cell pairs in juvenile rat barrel cortex: physiology and anatomy of interlaminar signalling within a cortical column. The Journal of physiology *538*, 803-822.

Felleman, D.J., and Van Essen, D.C. (1991). Distributed hierarchical processing in the primate cerebral cortex. Cereb Cortex *1*, 1-47.

Ferster, D., and Lindstrom, S. (1985). Synaptic excitation of neurones in area 17 of the cat by intracortical axon collaterals of cortico-geniculate cells. The Journal of physiology *367*, 233-252.

Fino, E., and Yuste, R. (2011). Dense Inhibitory Connectivity in Neocortex. Neuron *69*, 1188-1203.

Fox, M.D., Snyder, A.Z., Vincent, J.L., and Raichle, M.E. (2007). Intrinsic fluctuations within cortical systems account for intertrial variability in human behavior. Neuron *56*, 171-184.

Freund, T.F., and Buzsaki, G. (1996). Interneurons of the hippocampus. Hippocampus *6*, 347-470.

Freund, T.F., and Katona, I. (2007). Perisomatic inhibition. Neuron *56*, 33-42.

Galarreta, M., Erdelyi, F., Szabo, G., and Hestrin, S. (2004). Electrical coupling among irregular-spiking GABAergic interneurons expressing cannabinoid receptors. J Neurosci *24*, 9770-9778.

Galarreta, M., and Hestrin, S. (1999). A network of fast-spiking cells in the neocortex connected by electrical synapses. Nature *402*, 72-75.

Galarreta, M., and Hestrin, S. (2001a). Electrical synapses between GABA-releasing interneurons. Nat Rev Neurosci *2*, 425-433.

Galarreta, M., and Hestrin, S. (2001b). Spike transmission and synchrony detection in networks of GABAergic interneurons. Science *292*, 2295-2299.

Gawne, T.J., and Richmond, B.J. (1993). How independent are the messages carried by adjacent inferior temporal cortical neurons? J Neurosci *13*, 2758-2771.

Gibson, J.R., Beierlein, M., and Connors, B.W. (1999). Two networks of electrically coupled inhibitory neurons in neocortex. Nature *402*, 75-79.

Gibson, J.R., Beierlein, M., and Connors, B.W. (2005). Functional properties of electrical synapses between inhibitory interneurons of neocortical layer 4. J Neurophysiol *93*, 467-480.

Gilbert, C.D., and Wiesel, T.N. (1983). Functional organization of the visual cortex. Progress in brain research *58*, 209-218.

Gupta, A., Wang, Y., and Markram, H. (2000). Organizing principles for a diversity of GABAergic interneurons and synapses in the neocortex. Science *287*, 273-278.

Hahn, T.T., Sakmann, B., and Mehta, M.R. (2006). Phase-locking of hippocampal interneurons' membrane potential to neocortical up-down states. Nature neuroscience *9*, 1359-1361.

Hahn, T.T., Sakmann, B., and Mehta, M.R. (2007). Differential responses of hippocampal subfields to cortical up-down states. Proc Natl Acad Sci U S A *104*, 5169-5174.

Halabisky, B., Shen, F., Huguenard, J.R., and Prince, D.A. (2006). Electrophysiological classification of somatostatin-positive interneurons in mouse sensorimotor cortex. J Neurophysiol *96*, 834-845.

Hasenstaub, A., Shu, Y., Haider, B., Kraushaar, U., Duque, A., and McCormick, D.A. (2005). Inhibitory postsynaptic potentials carry synchronized frequency information in active cortical networks. Neuron *47*, 423-435.

Hertz, J. (2010). Cross-correlations in high-conductance states of a model cortical network. Neural Comput *22*, 427-447.

Hestrin, S., and Galarreta, M. (2005). Synchronous versus asynchronous transmitter release: a tale of two types of inhibitory neurons. Nat Neurosci *8*, 1283-1284.

Holmgren, C., Harkany, T., Svennenfors, B., and Zilberter, Y. (2003). Pyramidal cell communication within local networks in layer 2/3 of rat neocortex. J Physiol *551*, 139-153.

Howard, A., Tamas, G., and Soltesz, I. (2005). Lighting the chandelier: new vistas for axo-axonic cells. Trends in neurosciences *28*, 310-316.

Hu, H., Ma, Y., and Agmon, A. (2011). Submillisecond firing synchrony between different subtypes of cortical interneurons connected chemically but not electrically. J Neurosci *31*, 3351-3361.

Hubel, D.H., and Wiesel, T.N. (1959). Receptive fields of single neurones in the cat's striate cortex. The Journal of physiology *148*, 574-591.

Hull, C., Isaacson, J.S., and Scanziani, M. (2009). Postsynaptic mechanisms govern the differential excitation of cortical neurons by thalamic inputs. J Neurosci *29*, 9127-9136.

Isomura, Y., Sirota, A., Ozen, S., Montgomery, S., Mizuseki, K., Henze, D.A., and Buzsaki, G. (2006). Integration and segregation of activity in entorhinal-hippocampal subregions by neocortical slow oscillations. Neuron *52*, 871-882.

Kaminski, J., Wrobel, A., and Kublik, E. (2011). Gap junction blockade eliminates supralinear summation of fast (>200Hz) oscillatory components during sensory integration in the rat barrel cortex. Brain Res Bull.

Kampa, B.M., Letzkus, J.J., and Stuart, G.J. (2006). Cortical feed-forward networks for binding different streams of sensory information. Nat Neurosci *9*, 1472-1473.

Kandel, E.R. (2006). In search of memory : the emergence of a new science of mind, 1st edn (New York, W. W. Norton & Company).

Kapfer, C., Glickfeld, L.L., Atallah, B.V., and Scanziani, M. (2007). Supralinear increase of recurrent inhibition during sparse activity in the somatosensory cortex. Nature neuroscience *10*, 743-753.

Karube, F., Kubota, Y., and Kawaguchi, Y. (2004). Axon branching and synaptic bouton phenotypes in GABAergic nonpyramidal cell subtypes. J Neurosci *24*, 2853-2865.

Katona, I., Acsady, L., and Freund, T.F. (1999). Postsynaptic targets of somatostatin-immunoreactive interneurons in the rat hippocampus. Neuroscience *88*, 37-55.

Kätzel, D., Zemelman, B.V., Buetfering, C., Wölfel, M., and Miesenböck, G. (2010). The columnar and laminar organization of inhibitory connections to neocortical excitatory cells. Nature Neuroscience *14*, 100-107.

Kawaguchi, Y., Aosaki, T., and Kubota, Y. (1997). Cholinergic and GABAergic interneurons in the striatum. Nihon shinkei seishin yakurigaku zasshi = Japanese journal of psychopharmacology *17*, 87-90.

Kawaguchi, Y., and Kondo, S. (2002). Parvalbumin, somatostatin and cholecystokinin as chemical markers for specific GABAergic interneuron types in the rat frontal cortex. J Neurocytol *31*, 277-287.

Kawaguchi, Y., and Kubota, Y. (1997). GABAergic cell subtypes and their synaptic connections in rat frontal cortex. Cereb Cortex *7*, 476-486.

Klausberger, T., Magill, P.J., Marton, L.F., Roberts, J.D., Cobden, P.M., Buzsaki, G., and Somogyi, P. (2003). Brain-state- and cell-type-specific firing of hippocampal interneurons in vivo. Nature *421*, 844-848.

Kosaka, T., Katsumaru, H., Hama, K., Wu, J.Y., and Heizmann, C.W. (1987). GABAergic neurons containing the Ca2+-binding protein parvalbumin in the rat hippocampus and dentate gyrus. Brain Res *419*, 119-130.

Kozloski, J., Hamzei-Sichani, F., and Yuste, R. (2001). Stereotyped position of local synaptic targets in neocortex. Science *293*, 868-872.

Kwong, K.K., Belliveau, J.W., Chesler, D.A., Goldberg, I.E., Weisskoff, R.M., Poncelet, B.P., Kennedy, D.N., Hoppel, B.E., Cohen, M.S., Turner, R., *et al.* (1992). Dynamic magnetic resonance imaging of human brain activity during primary sensory stimulation. Proceedings of the National Academy of Sciences of the United States of America *89*, 5675-5679.

Lampl, I., Reichova, I., and Ferster, D. (1999). Synchronous membrane potential fluctuations in neurons of the cat visual cortex. Neuron *22*, 361-374.

Land, P.W., Buffer, S.A., Jr., and Yaskosky, J.D. (1995). Barreloids in adult rat thalamus: three-dimensional architecture and relationship to somatosensory cortical barrels. The Journal of comparative neurology *355*, 573-588.

Lewis, T.J., and Rinzel, J. (2003). Dynamics of spiking neurons connected by both inhibitory and electrical coupling. J Comput Neurosci *14*, 283-309.

Lisman, J., and Buzsaki, G. (2008). A neural coding scheme formed by the combined function of gamma and theta oscillations. Schizophr Bull *34*, 974-980.

Lopez-Bendito, G., Sturgess, K., Erdelyi, F., Szabo, G., Molnar, Z., and Paulsen, O. (2004). Preferential origin and layer destination of GAD65-GFP cortical interneurons. Cereb Cortex *14*, 1122-1133.

Lorente de No, R. (1922a). La corteza cerebral del ratón (Primera contribución – La corteza acústica). Trabajos del Laboratorio de Investigaciones Biológicas *20*, 41-78.

Lorente de No, R. (1922b). La corteza cerebral del raton. Primera contribucion. La corteza acustica. Trab Lab Invest (Madrid) *20*, 41-104.

Lorente de No, R., and Condouris, G.A. (1959). Decremental Conduction in Peripheral Nerve. Integration of Stimuli in the Neuron. Proceedings of the National Academy of Sciences of the United States of America *45*, 592-617.

Lubke, J., and Feldmeyer, D. (2007). Excitatory signal flow and connectivity in a cortical column: focus on barrel cortex. Brain structure & function *212*, 3-17.

Luczak, A., Bartho, P., Marguet, S.L., Buzsaki, G., and Harris, K.D. (2007). Sequential structure of neocortical spontaneous activity in vivo. Proceedings of the National Academy of Sciences of the United States of America *104*, 347-352.

MacLean, J.N., Watson, B.O., Aaron, G.B., and Yuste, R. (2005). Internal dynamics determine the cortical response to thalamic stimulation. Neuron *48*, 811-823.

Mahon, S., Deniau, J.M., and Charpier, S. (2001). Relationship between EEG potentials and intracellular activity of striatal and cortico-striatal neurons: an in vivo study under different anesthetics. Cereb Cortex *11*, 360-373.

Mann, E.O., and Paulsen, O. (2005). Mechanisms underlying gamma ('40 Hz') network oscillations in the hippocampus--a mini-review. Progress in biophysics and molecular biology *87*, 67-76.

Mann, E.O., Radcliffe, C.A., and Paulsen, O. (2005). Hippocampal gamma-frequency oscillations: from interneurones to pyramidal cells, and back. The Journal of physiology *562*, 55-63.

Markram, H., Toledo-Rodriguez, M., Wang, Y., Gupta, A., Silberberg, G., and Wu, C. (2004). Interneurons of the neocortical inhibitory system. Nature reviews *5*, 793-807.

Marshall, W.H., Woolsey, C.N., and Bard, P. (1937). Cortical Representation of Tactile Sensibility as Indicated by Cortical Potentials. Science *85*, 388-390.

McClurkin, J.W., Optican, L.M., Richmond, B.J., and Gawne, T.J. (1991). Concurrent processing and complexity of temporally encoded neuronal messages in visual perception. Science *253*, 675-677.

McCormick, D.A., Connors, B.W., Lighthall, J.W., and Prince, D.A. (1985). Comparative electrophysiology of pyramidal and sparsely spiny stellate neurons of the neocortex. J Neurophysiol *54*, 782-806.

McGarry, L.M., Packer, A.M., Fino, E., Nikolenko, V., Sippy, T., and Yuste, R. (2010). Quantitative classification of somatostatin-positive neocortical interneurons identifies three interneuron subtypes. Front Neural Circuits *4*, 12.

Merriam, E.B., Netoff, T.I., and Banks, M.I. (2005). Bistable network behavior of layer I interneurons in auditory cortex. J Neurosci *25*, 6175-6186.

Miles, R., Toth, K., Gulyas, A.I., Hajos, N., and Freund, T.F. (1996). Differences between somatic and dendritic inhibition in the hippocampus. Neuron *16*, 815-823.

Monyer, H., and Markram, H. (2004). Interneuron Diversity series: Molecular and genetic tools to study GABAergic interneuron diversity and function. Trends in neurosciences *27*, 90-97.

Mountcastle, V.B. (1978). An organizing principle for cerebral function: the unit module and the distributed system. In The mindful brain : cortical organization and the group-selective theory of higher brain function (Cambridge, MIT Press), p. 100p.

Mountcastle, V.B., and Powell, T.P. (1959). Neural mechanisms subserving cutaneous sensibility, with special reference to the role of afferent inhibition in sensory perception and discrimination. Bulletin of the Johns Hopkins Hospital *105*, 201-232.

Nikolenko, V., Watson, B.O., Araya, R., Woodruff, A., Peterka, D.S., and Yuste, R. (2008). SLM Microscopy: Scanless Two-Photon Imaging and Photostimulation with Spatial Light Modulators. Front Neural Circuits *2*, 5.

Nomura, M., Fukai, T., and Aoyagi, T. (2003). Synchrony of fast-spiking interneurons interconnected by GABAergic and electrical synapses. Neural Comput *15*, 2179-2198.

Oliva, A.A., Jr., Jiang, M., Lam, T., Smith, K.L., and Swann, J.W. (2000). Novel hippocampal interneuronal subtypes identified using transgenic mice that express green fluorescent protein in GABAergic interneurons. J Neurosci *20*, 3354-3368.

Oswald, A.M., Doiron, B., Rinzel, J., and Reyes, A.D. (2009). Spatial profile and differential recruitment of GABAB modulate oscillatory activity in auditory cortex. J Neurosci *29*, 10321-10334.

Packer, A., and Yuste, R. (2011). Dense, unspecific connectivity of neocortical parvalbumin-positive interneurons: a canonical microcircuit for inhibition? In preparation.

Penfield, W., and Rasmussen, T. (1950). The cerebral cortex of man; a clinical study of localization of function (New York,, Macmillan).

Petersen, C.C., Grinvald, A., and Sakmann, B. (2003a). Spatiotemporal dynamics of sensory responses in layer 2/3 of rat barrel cortex measured in vivo by voltage-sensitive dye imaging combined with whole-cell voltage recordings and neuron reconstructions. J Neurosci *23*, 1298-1309.

Petersen, C.C., Hahn, T.T., Mehta, M., Grinvald, A., and Sakmann, B. (2003b). Interaction of sensory responses with spontaneous depolarization in layer 2/3 barrel cortex. Proceedings of the National Academy of Sciences of the United States of America *100*, 13638-13643.

Pfeuty, B., Mato, G., Golomb, D., and Hansel, D. (2003). Electrical synapses and synchrony: the role of intrinsic currents. J Neurosci *23*, 6280-6294.

Pouille, F., and Scanziani, M. (2001). Enforcement of temporal fidelity in pyramidal cells by somatic feed-forward inhibition. Science *293*, 1159-1163.

Rall, W. (1959). Branching dendritic trees and motoneuron membrane resistivity. Experimental neurology *1*, 491-527.

Ramón y Cajal, S., DeFelipe, J., and Jones, E.G. (1988). Cajal on the cerebral cortex : an annotated translation of the complete writings (New York, Oxford University Press).

Renart, A., de la Rocha, J., Bartho, P., Hollender, L., Parga, N., Reyes, A., and Harris, K.D. (2010). The Asynchronous State in Cortical Circuits. Science *327*, 587-590.

Reyes, A., and Sakmann, B. (1999). Developmental switch in the short-term modification of unitary EPSPs evoked in layer 2/3 and layer 5 pyramidal neurons of rat neocortex. J Neurosci *19*, 3827-3835.

Rudolph, M., Pelletier, J.G., Pare, D., and Destexhe, A. (2005). Characterization of synaptic conductances and integrative properties during electrically induced EEG-activated states in neocortical neurons in vivo. J Neurophysiol *94*, 2805-2821.

Rudy, B., Fishell, G., Lee, S., and Hjerling-Leffler, J. (2011). Three groups of interneurons account for nearly 100% of neocortical GABAergic neurons. Dev Neurobiol *71*, 45-61.

Sanchez-Vives, M.V., and McCormick, D.A. (2000). Cellular and network mechanisms of rhythmic recurrent activity in neocortex. Nature neuroscience *3*, 1027-1034.

Saraga, F., Ng, L., and Skinner, F.K. (2006). Distal gap junctions and active dendrites can tune network dynamics. J Neurophysiol *95*, 1669-1682.

Shadlen, M.N., and Newsome, W.T. (1998). The variable discharge of cortical neurons: implications for connectivity, computation, and information coding. J Neurosci *18*, 3870-3896.

Shepherd, G.M., Pologruto, T.A., and Svoboda, K. (2003). Circuit analysis of experience-dependent plasticity in the developing rat barrel cortex. Neuron *38*, 277-289.

Shu, Y., Hasenstaub, A., and McCormick, D.A. (2003). Turning on and off recurrent balanced cortical activity. Nature *423*, 288-293.

Silberberg, G., and Markram, H. (2007). Disynaptic inhibition between neocortical pyramidal cells mediated by Martinotti cells. Neuron *53*, 735-746.

Singer, W. (2009). Distributed processing and temporal codes in neuronal networks. Cogn Neurodyn *3*, 189-196.

Smith, S.L., and Häusser, M. (2010). Parallel processing of visual space by neighboring neurons in mouse visual cortex. Nature Neuroscience *13*, 1144-1149.

Somogyi, P., and Klausberger, T. (2005). Defined types of cortical interneurone structure space and spike timing in the hippocampus. J Physiol *562*, 9-26.

Somogyi, P., Tamas, G., Lujan, R., and Buhl, E.H. (1998). Salient features of synaptic organisation in the cerebral cortex. Brain research *26*, 113-135.

Sompolinsky, H., Yoon, H., Kang, K., and Shamir, M. (2001). Population coding in neuronal systems with correlated noise. Phys Rev E Stat Nonlin Soft Matter Phys *64*, 051904.

Staiger, J.F., Kotter, R., Zilles, K., and Luhmann, H.J. (2000). Laminar characteristics of functional connectivity in rat barrel cortex revealed by stimulation with caged-glutamate. Neurosci Res *37*, 49-58.

Steriade, M., Timofeev, I., and Grenier, F. (2001). Natural waking and sleep states: a view from inside neocortical neurons. J Neurophysiol *85*, 1969-1985.

Stuart, G.J., Dodt, H.U., and Sakmann, B. (1993). Patch-clamp recordings from the soma and dendrites of neurons in brain slices using infrared video microscopy. Pflugers Arch *423*, 511-518.

Sun, Q.Q., Huguenard, J.R., and Prince, D.A. (2006). Barrel cortex microcircuits: thalamocortical feedforward inhibition in spiny stellate cells is mediated by a small number of fast-spiking interneurons. J Neurosci *26*, 1219-1230.

Tamamaki, N., Yanagawa, Y., Tomioka, R., Miyazaki, J., Obata, K., and Kaneko, T. (2003). Green fluorescent protein expression and colocalization with calretinin, parvalbumin, and somatostatin in the GAD67-GFP knock-in mouse. The Journal of comparative neurology *467*, 60-79.

Tamas, G., Buhl, E.H., Lorincz, A., and Somogyi, P. (2000). Proximally targeted GABAergic synapses and gap junctions synchronize cortical interneurons. Nat Neurosci *3*, 366-371.

Tan, Z., Hu, H., Huang, Z.J., and Agmon, A. (2008). Robust but delayed thalamocortical activation of dendritic-targeting inhibitory interneurons. Proc Natl Acad Sci U S A *105*, 2187-2192.

Thomson, A.M., and Deuchars, J. (1997). Synaptic interactions in neocortical local circuits: dual intracellular recordings in vitro. Cereb Cortex *7*, 510-522.

Thomson, A.M., West, D.C., Hahn, J., and Deuchars, J. (1996). Single axon IPSPs elicited in pyramidal cells by three classes of interneurones in slices of rat neocortex. J Physiol *496 (Pt 1)*, 81-102.

Vaadia, E., Haalman, I., Abeles, M., Bergman, H., Prut, Y., Slovin, H., and Aertsen, A. (1995). Dynamics of neuronal interactions in monkey cortex in relation to behavioural events. Nature *373*, 515-518.

Vervaeke, K., Lorincz, A., Gleeson, P., Farinella, M., Nusser, Z., and Silver, R.A. (2010). Rapid Desynchronization of an Electrically Coupled Interneuron Network with Sparse Excitatory Synaptic Input. Neuron *67*, 435-451.

Vogels, T.P., and Abbott, L.F. (2009). Gating multiple signals through detailed balance of excitation and inhibition in spiking networks. Nat Neurosci *12*, 483-491.

Vogelstein, J.T., Packer, A.M., Machado, T.A., Sippy, T., Babadi, B., Yuste, R., and Paninski, L. (2010). Fast nonnegative deconvolution for spike train inference from population calcium imaging. J Neurophysiol *104*, 3691-3704.

Wang, Y., Toledo-Rodriguez, M., Gupta, A., Wu, C., Silberberg, G., Luo, J., and Markram, H. (2004). Anatomical, physiological and molecular properties of Martinotti cells in the somatosensory cortex of the juvenile rat. J Physiol *561*, 65-90.

Weinberger, D.R., Berman, K.F., and Zec, R.F. (1986). Physiologic dysfunction of dorsolateral prefrontal cortex in schizophrenia. I. Regional cerebral blood flow evidence. Archives of general psychiatry *43*, 114-124.

Welker, C. (1976). Receptive fields of barrels in the somatosensory neocortex of the rat. The Journal of comparative neurology *166*, 173-189.

Whittington, M.A., and Traub, R.D. (2003). Interneuron diversity series: inhibitory interneurons and network oscillations in vitro. Trends Neurosci *26*, 676-682.

Wilson, C.J., and Groves, P.M. (1981). Spontaneous firing patterns of identified spiny neurons in the rat neostriatum. Brain research *220*, 67-80.

Wilson, C.J., and Kawaguchi, Y. (1996). The origins of two-state spontaneous membrane potential fluctuations of neostriatal spiny neurons. J Neurosci *16*, 2397-2410.

Woolsey, T.A., and Van der Loos, H. (1970). The structural organization of layer IV in the somatosensory region (SI) of mouse cerebral cortex. The description of a cortical field composed of discrete cytoarchitectonic units. Brain research *17*, 205-242.

Xu, X., Roby, K.D., and Callaway, E.M. (2010). Immunochemical characterization of inhibitory mouse cortical neurons: three chemically distinct classes of inhibitory cells. J Comp Neurol *518*, 389-404.

Yoshimura, Y., and Callaway, E.M. (2005). Fine-scale specificity of cortical networks depends on inhibitory cell type and connectivity. Nat Neurosci *8*, 1552-1559.

Yoshimura, Y., Dantzker, J.L.M., and Callaway, E.M. (2005). Excitatory cortical neurons form fine-scale functional networks. Nature *433*, 868-873.

Yuste, R., and Katz, L.C. (1991). Control of postsynaptic Ca2+ influx in developing neocortex by excitatory and inhibitory neurotransmitters. Neuron *6*, 333-344.

Yuste, R., Peinado, A., and Katz, L.C. (1992). Neuronal domains in developing neocortex. Science *257*, 665-669.

Yuste, R., and Tank, D.W. (1996). Dendritic integration in mammalian neurons, a century after Cajal. Neuron *16*, 701-716.

Zhang, F., Gradinaru, V., Adamantidis, A.R., Durand, R., Airan, R.D., de Lecea, L., and Deisseroth, K. (2010). Optogenetic interrogation of neural circuits: technology for probing mammalian brain structures. Nat Protoc *5*, 439-456.

Zhang, F., Wang, L.P., Brauner, M., Liewald, J.F., Kay, K., Watzke, N., Wood, P.G., Bamberg, E., Nagel, G., Gottschalk, A., *et al.* (2007). Multimodal fast optical interrogation of neural circuitry. Nature *446*, 633-639.

Zohary, E., Shadlen, M.N., and Newsome, W.T. (1994). Correlated neuronal discharge rate and its implications for psychophysical performance. Nature *370*, 140-143.